

Beyond the Standard Model contributions to dipole moments

Oscar Vives^a and Nicola Valori^a

^aInstitut de Física Corpuscular (CSIC-Universitat de València), Departament de Física Teòrica, Dr. Moliner 50, E-46100 Burjassot (València), Spain

© 20xx Elsevier Ltd. All rights reserved.

Chapter Article tagline: update of previous edition, reprint.

Contents

Objectives	1
1 Introduction	2
2 Dipole moments and the search for new physics	2
3 Dipole moments beyond the Standard Model	5
3.1 Two-Higgs doublet models	7
3.2 Supersymmetry	11
3.3 Extra $U(1)$ gauge symmetries	14
3.4 Standard Model Effective Field Theory	15
4 Dipole observables	17
4.1 Muon Anomalous Magnetic Moment	17
4.2 Electric Dipole Moments	19
4.3 Flavor-Changing Dipole Transitions	20
5 Conclusions	22
Acknowledgments	23
References	23

Abstract

The goal of this work is to provide a pedagogical introduction to dipole moments and dipole transitions in theories beyond the Standard Model, with a focus on the lepton sector. We emphasize the exceptional sensitivity of dipole observables to new physics, analyzing the most sensitive processes, such as the muon anomalous magnetic moment, the electric dipole moment of the electron, and the branching ratio $\text{BR}(\mu \rightarrow e\gamma)$. This review is intended for PhD students, early-career researchers, and anyone entering the field for the first time. It does not aim to provide a complete overview of all models in the literature, but rather to serve as an accessible guide, using simple and representative examples from the most well-studied extensions of the Standard Model.

Keywords: Review, Anomalous Magnetic Moment, Electric Dipole Moment, Muon to electron photon, New Physics, CP violation, Flavor changing neutral currents, Experimental sensitivity

Objectives

- In this review, we aim to present some of the key ideas related to dipole observables and their power in probing new physics (NP). We discuss why dipole moments are among the most sensitive observables for detecting physics beyond the Standard Model (SM), and identify, based on both experimental and theoretical considerations, the most promising dipole observables for near-future exploration.
- We emphasize that all dipole observables are deeply interconnected and offer a unified framework for their treatment. General expressions for the dipole matrix at one-loop level are provided, along with a discussion of particularly relevant two-loop contributions, such as the Barr-Zee diagrams, which play an important role in models with small Yukawa couplings.
- This formalism is then applied to study the main features of dipole contributions in several well-known extensions of the SM: two-Higgs-doublet models (2HDM), supersymmetric models, theories with extra $U(1)$ gauge symmetries, and the Standard Model Effective Field Theory (SMEFT). Our focus is not on identifying the models that yield the largest contributions to dipole observables, but rather on illustrating the diverse types of new physics that can affect them.
- This is by no means an exhaustive list of SM extensions contributing to dipole transitions. Readers interested in further details are encouraged to consult the extensive literature and existing reviews. Below, we provide a selection of complementary works organized by topic, which may offer deeper insights. For a general overview on the physics of lepton dipole moments we refer the reader to the book [1]. For discussions on the muon's anomalous magnetic moment in and beyond the SM, see [2–4]. For electric dipole moments, detailed introductions to new physics contributions can be found in [5–7]. Finally, for a general overview of $\mu \rightarrow e$ transitions, see [8–10].

1 Introduction

Dipole moments, or dipole transitions, are quantities that characterize how fermions interact with external electromagnetic fields. Unlike the usual electromagnetic current, which describes the renormalizable interactions of the electromagnetic field, dipole moments arise from effective interactions associated with higher-dimensional operators. These operators are suppressed by the scale of physics associated to the loop and can be sensitive to the effects of heavy virtual particles predicted by many extensions of the SM. As we will discuss below, dipole operators can probe a broad range of physical phenomena, including Lepton Flavor Violation (LFV) and CP violation, making them powerful tools in the search for NP.

Indeed, dipole interactions have played, and continue to play, a pivotal role in testing the SM of particle physics and exploring physics beyond it across a wide range of energy scales. In the following, we focus on dipole observables in the leptonic sector, which are among the most sensitive probes for physics beyond the SM.

Within the leptonic sector, dipole observables can be categorized into three groups: gyromagnetic ratios (or g-factors), which are both experimentally measured and theoretically predicted with exceptional precision within the SM; electric dipole moments (EDMs), which violate CP symmetry and whose current experimental bounds lie many orders of magnitude above SM expectations; and lepton flavor transitions, which violate lepton flavor conservation and are strictly forbidden in the SM (neglecting neutrino masses), thus offering a clean window into potential NP.

The g-factor is defined as the proportionality constant between the magnetic moment ($\vec{\mu}$) and the spin (\vec{s}) of a fermion f with charge q and mass m : $\vec{\mu} = g q/(2m) \vec{s}$. The historical significance of the g-factor lies in its early role as a test of quantum theory. Dirac's relativistic theory of quantum mechanics famously predicted that the g-factor of a free, point-like fermion should be exactly 2. However, in 1948, Julian Schwinger computed the leading-order quantum correction to the electron's magnetic moment, arising from the exchange of a virtual photon, and found an additional term of α_{em}/π [11], where α_{em} is the electromagnetic fine structure constant. This correction explained the small, unexpected 0.12% excess observed in precision measurements of the electron's magnetic moment, a discrepancy referred to as the anomalous magnetic moment of the electron [12]. This extraordinary success established Quantum Electrodynamics as the correct theory for describing electromagnetic interactions, and quantum field theory as a general framework for the theory of elementary particles. It is now conventional to define the anomalous magnetic moment of a fermion f as: $a_f = (g_f - 2)/2$, which quantifies the deviation of g_f from the Dirac value of 2. Since then, anomalous magnetic moments have been measured with incredible accuracy, becoming the best measured quantity in the SM. Nowadays, the electron's g-factor is known with an accuracy of 0.13 ppb [13], and the muon's g factor with an accuracy of 0.19 ppm [14]. These measurements, along with the corresponding theoretical calculations at high orders, allow to probe the SM and search for extensions of it ¹. Given the exceptional sensitivity to NP and the current unresolved puzzles, as explained in Section 4.1, this work focuses mainly on the anomalous magnetic moment of the muon.

Similarly to magnetic moments, parametrizing the interaction between a particle with spin and a magnetic field, EDMs characterize the interaction between a fermion and an external electric field. In the non relativistic theory, they can be parametrized by $\mathcal{H}_{\text{int}} = -d_f \vec{E} \cdot \hat{s}$, where d_f is the EDM of the fermion. Given the fact that the spin \vec{s} is a pseudo-vector and the electric field \vec{E} is a vector, this interaction term violates parity (and more generally CP). The need for new sources of CP violation, other than the SM one, is well motivated by physical processes that requires physics beyond the SM, such as Baryogenesis. Theoretically, EDMs are particularly well-suited for CP violating NP searches because their SM contributions are extremely suppressed. Experiments looking for EDMs are sensitive to much larger values than those predicted by the SM, and would thus be able to unambiguously detect or constraint CP-odd new physics interactions. Indeed, within the SM, the lepton EDM appears only at four-loop order, predicting, for the electron, $d_e \sim 10^{-44} \text{ e} \cdot \text{cm}$ [19] ². These values are still very far from the corresponding experimental sensitivities, that place upper bounds of $d_e < 4.1 \times 10^{-30} \text{ e} \cdot \text{cm}$ at 90 % confidence level [21] .

Finally, the third class of dipole observables are lepton flavor-violating processes, such as $\mu \rightarrow e\gamma$, $\tau \rightarrow e\gamma$, and $\tau \rightarrow \mu\gamma$. In the SM with massive neutrinos, these transitions are extremely suppressed, with branching ratios scaling as $(m_\nu/M_W)^4$. Consequently, this results in $\text{Br}(\mu \rightarrow e\gamma) \sim 10^{-55} \div 10^{-54}$, far beyond the reach of even the most ambitious experimental efforts. As a result, any observation of LFV in dipole transitions would provide a clear and unambiguous signal of physics beyond the SM with new flavor structures. The experimental status as well as the theoretical predictions in the SM for the leptonic dipole observables are summarized in Table 1.

This work is organized as follow. In Section 2, we define the dipole operator and show how the various dipole observables are related to it. In Section 3, we provide general expressions for the dipole operator at one-loop level, along with selected two loop effects that maybe relevant. These expressions are then applied to illustrative examples of beyond the SM theories. In Section 4, we summarize the impact of such extensions of SM to dipole observables. Finally, in Section 5, we present our conclusions.

2 Dipole moments and the search for new physics

To understand the role and importance of dipoles in the search for NP, it is essential to express the relevant observables within the framework of Quantum Field Theory. In the flavor-diagonal sector, the most general Lorentz-invariant form of the fermion-photon amplitude at loop

¹There are potential discrepancies between the SM predictions and the experimental values of a_e and a_μ . For recent determinations of the SM value and discussions, see Refs. [15–18].

²However, the dominant contribution to the lepton EDM arises from long-distance effects, which have been evaluated using hadronic effective models [20]. These values are presented in Table 1.

Observable	Experiment	SM Prediction
a_e	$115\,965\,218.059(13) \times 10^{-11}$ [13]	$115\,965\,218.0252(95) \times 10^{-11}$ [$\alpha(\text{Rb})$] [17] $115\,965\,218.161(23) \times 10^{-11}$ [$\alpha(\text{Cs})$] [18]
a_μ	$116\,592\,059(22) \times 10^{-11}$ [14]	$116\,591\,810(43) \times 10^{-11}$ (e^+e^-) [15] $116\,592\,019(38) \times 10^{-11}$ (BMW) [16]
$ d_e $	$< 4.1 \times 10^{-30}$ e cm [21]	$\sim 1 \times 10^{-39}$ e cm [20]
$ d_\mu $	$< 1.8 \times 10^{-19}$ e cm [22]	$\sim 1 \times 10^{-38}$ e cm [20]
$ d_\tau $	$\lesssim 1 \times 10^{-17}$ e cm [23]	$\sim 1 \times 10^{-37}$ e cm [20]
$\text{BR}(\mu \rightarrow e\gamma)$	$< 3.1 \times 10^{-13}$ [24]	$\sim 10^{-55} \div 10^{-54}$
$\text{BR}(\tau \rightarrow e\gamma)$	$< 3.3 \times 10^{-8}$ [25]	$\sim 10^{-55} \div 10^{-54}$
$\text{BR}(\tau \rightarrow \mu\gamma)$	$< 4.4 \times 10^{-8}$ [25]	$\sim 10^{-55} \div 10^{-54}$

Table 1: Summary of experimental measurements and SM predictions for dipole-related observables in the lepton sector. The SM values for a_e use both Rubidium and Cesium determinations of α_{em} . For a_μ , we show predictions from e^+e^- data and lattice QCD (BMW). All upper bounds are quoted at 90% C.L.

level reads

$$i\mathcal{M} = -ie Q_\ell A_\mu(q) \bar{u}_l(p') \Gamma^\mu(q^2) u_l(p), \quad (1)$$

where Γ^μ generalizes the standard tree-level Lorentz vector, γ^μ , as follows³,

$$\Gamma^\mu = F_1(q^2) \gamma^\mu + F_2(q^2) \frac{i\sigma^{\mu\nu} q_\nu}{2m_\ell} - F_3(q^2) \gamma_5 \sigma^{\mu\nu} q_\nu. \quad (2)$$

This parametrization holds to all orders in perturbation theory. The first form factor $F_1(q^2)$ is associated to the renormalization of the electromagnetic current, while the other two leads to the definition of a_ℓ and d_ℓ as⁴:

$$a_\ell = F_2(0); \quad d_\ell/e = F_3(0), \quad (3)$$

where we notice that the a_ℓ is dimensionless quantity while d_ℓ has a mass dimension of Energy^{-1} .

In order to predict contributions to dipole observables in extensions of the SM, we define the dipole operator in the low energy effective Lagrangian:

$$\mathcal{L} \supset \frac{e}{8\pi^2} C_{ji} (\bar{\ell}_j \sigma_{\mu\nu} P_R \ell_i) F^{\mu\nu} + \text{h.c.}, \quad (4)$$

where $F^{\mu\nu} = \partial^\mu A^\nu - \partial^\nu A^\mu$ is the electromagnetic field strength tensor and the Wilson coefficient $C_{\ell_j \ell_i}$ is a matrix in flavor space of mass dimension Energy^{-1} that we call the dipole matrix.

Therefore, in terms of the above Wilson coefficients, the NP contribution to the anomalous magnetic moment, Δa_ℓ , and the electric dipole moment, d_ℓ , are given by,

$$\Delta a_{\ell_i} = \frac{m_{\ell_i}}{2\pi^2} \text{Re}(C_{ii}), \quad d_{\ell_i} = -\frac{e}{4\pi^2} \text{Im}(C_{ii}). \quad (5)$$

Similarly, the off-diagonal entries of the dipole matrix describe LFV transitions,

$$\text{BR}(\ell_j \rightarrow \ell_i \gamma) = \frac{3\alpha_{\text{em}}}{\pi G_F^2 m_{\ell_j}^2} (|C_{ji}|^2 + |C_{ij}|^2). \quad (6)$$

At this point, we can understand why dipole transitions are so effective in the search for extensions of the SM. The main reason is that dipole transitions are induced by a dimension-five operator and must appear at loop level in any renormalizable theory, such as the SM. This makes them sensitive to heavy virtual particles, such as those predicted by many SM extensions, even if those particles are too massive to

³An additional term, the so called anapole moment, is allowed by the Lorentz structure of the amplitude. However it does not represent a well-defined observable [26].

⁴From now on, we simply rewrite $f = \ell$ to stress the fact that we refer to lepton quantities.

be directly produced in colliders. Figure 1 shows a generic topology representing a one-loop contribution to the dipole operator. Internal particles in the loop must be chosen according to the Feynman rules of the theory.

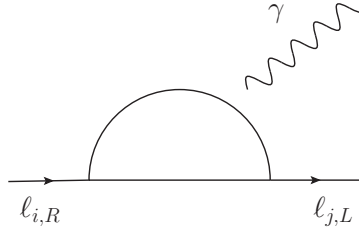


Fig. 1: Representative topology for a one-loop contribution to the dipole observables. i, j refer to the flavor indices while R, L refer to the chiral component of the external fermions

A second relevant aspect of dipole physics is the relationship between dipole and mass operators. Indeed, both of them require a chirality flip, i.e. transitions between left- and right-handed leptons, so that they must be generated by Lagrangian terms that break the chiral symmetry. In the SM, this is carried out only by the Yukawa sector and the Higgs mechanism. This fact guarantees that any contribution to dipole amplitudes is proportional to the SM fermion mass itself. However, due to the mysterious nature of the fermion masses hierarchy, many beyond the SM theories introduce new sources of chiral symmetry breakings, so that contributions to dipole operators may be proportional to the mass of new heavy states.

In addition to this, if we remove the external photon from the process in Figure 1, we obtain a loop correction to the chirality-changing two-point function. This corresponds to a loop correction to the mass, involving exactly the same interactions and states as the dipole operator. If we enhance the dipole contribution by means of heavy fermions in the loop, we expect, by dimensional arguments, that the NP correction to the mass to be of order, $\Delta m_\ell \sim G M_F$ with G the relevant combination of couplings and loop factors from the new interactions and M_F a heavy fermion mass. Assuming that the loop correction is not larger than the tree-level fermion mass⁵, we would expect $G M_F \lesssim m_\ell$. Then, this would impose an additional restriction, $\Delta a_\ell \sim G m_\ell M_F / M_F^2 \lesssim m_\ell^2 / M_F^2$ and similarly, under certain assumptions, for other dipole observables. The interplay between masses and dipoles plays a crucial role in determining the sensitivity of these observables to NP, both from the experimental and theoretical perspectives. In particular, anomalous magnetic moments and EDMs are given by the real or imaginary part of the same flavor-diagonal Wilson coefficient, in the basis of real and diagonal charged lepton masses. This implies that contributions to both the dipole matrix and the fermion masses must be taken into account to properly define anomalous magnetic moments and EDMs in the basis of real masses and extract the "observable" dipole moments⁶. In the models considered in this review, this issue must be addressed when the loop correction to the mass is of the same order as the tree-level mass, requiring a rephasing of the total mass to extract the observable EDM and magnetic moment values [28, 29].

These properties are particularly relevant in the study of anomalous magnetic moments. From an experimental point of view, it is much easier to work with first generation (stable) fermions, making the electron anomalous magnetic moment more precisely measured than the muon magnetic moment, as shown in Table 1. Moreover, as already said, the SM theoretical predictions for these anomalous magnetic moments are known with comparable precision to the experimental measurements in both cases. Therefore, at first sight, it may seem that the electron is more sensitive to NP contributions than the muon. However, this is not always the case.

Assuming that NP contributions to the anomalous magnetic moment arise at the one-loop level, the chirality change is proportional to the correction to the lepton mass Δm_ℓ . Then, from dimensional analysis and using Eq. (5), we find

$$\Delta a_\ell \sim \beta \frac{m_\ell^2}{\Lambda_{\text{NP}}^2}. \quad (7)$$

where Λ_{NP} is the scale of NP in the loop and $\beta \sim \Delta m_\ell / m_\ell$ at most $O(1)$ to respect $\Delta m_\ell \lesssim m_\ell$. Thus, assuming a similar β factor, the ratio of NP contributions to a_μ and a_e is given by

$$\frac{\Delta a_\mu}{\Delta a_e} \sim \frac{m_\mu^2}{m_e^2} = 4 \times 10^4. \quad (8)$$

⁵This is a naturalness issue. In a strictly technical sense, there is no problem with $\Delta m_\ell > m_\ell$, as we can always cancel this large contribution by an appropriate tuning of the tree-level mass.

⁶Dipole moments are not strictly basis-independent observables, but since they are extracted from physical processes, they can be embedded in weak basis invariants—typically by combining with chirality-changing operators like fermion masses. See [27] for a formal treatment.

This factor compensates for the difference in the current experimental sensitivities of the muon and electron anomalous magnetic moments. If we take the experimental uncertainties as shown in Table 1, we obtain,

$$\frac{\delta a_\mu^{\text{exp}}}{\delta a_e^{\text{exp}}} \sim 10^3. \quad (9)$$

This implies that, given the current experimental precision, the muon anomalous magnetic moment can probe energy scales roughly one order of magnitude higher than those accessible via the electron.

The situation is quite different for EDMs. Experimental sensitivity is significantly higher for the electron⁷, with $|d_e| < 4.1 \times 10^{-30}$ e cm, compared to $|d_\mu| < 1.8 \times 10^{-19}$ e cm. However, by applying an argument similar to that used for the anomalous magnetic moment, NP contributions are proportional to $m_\ell/\Lambda_{\text{NP}}^2$, leading to,

$$\frac{\Delta d_\mu}{\Delta d_e} \sim \frac{m_\mu}{m_e} = 2 \times 10^2. \quad (10)$$

Therefore, the electron EDM can probe energy scales that are a factor 5×10^4 larger than the muon EDM.

So, it is clear d_e will remain the main actor in the search for CP violating NP for the foreseeable future, even taking into account the suppression due to the small mass of the electron.

On the other hand, when exploring off-diagonal dipole transitions, the only viable options are muon or third-generation decays. In this case, muon decays are much better constrained experimentally than tau decays, with $\text{BR}(\mu^+ \rightarrow e^+ \gamma) < 3.1 \times 10^{-13}$ while $\text{BR}(\tau \rightarrow e \gamma) < 3.3 \times 10^{-8}$ (both at 90% Confidence Level). Therefore, there is no doubt that the key processes in flavor off-diagonal transitions will be muon decays, as $\mu \rightarrow e \gamma$, $\mu \rightarrow e e e$ or $\mu - e$ transitions in nuclei⁸.

3 Dipole moments beyond the Standard Model

Despite the tremendous success of the SM in explaining a wide range of phenomena, we remain convinced that NP must exist at high energies to address the various unanswered questions it leaves open. This NP involves new states or interactions that have yet to be detected, either due to experimental limitations or because these states are too heavy to be produced at current facilities.

Nevertheless, any contribution from NP is inherently present, most likely at the loop level, in any measured observable. If NP exists, then by comparing a precisely predicted observable with a sufficiently accurate experimental measurement, we should be able to identify discrepancies that indicate the incompleteness of our theory. Dipole transitions are the best example of this as they are loop processes in the SM. Consequently, NP contributions can compete on equal footing.

NP models are usually based on the introduction of new particles and interactions beyond the SM of particle physics, which, in a renormalizable theory, can be parametrized according to the following Lagrangian:

$$\mathcal{L} \supset -(y_{R,L})_{ij} S \bar{\ell}_i P_{R,L} F_j + (g_{R,L})_{ij} \bar{\ell}_i \gamma_\mu P_{R,L} F_j V^\mu + \text{h.c.} \quad (11)$$

where ℓ and A^μ are the SM leptons and electromagnetic field, while F_k (fermion), S (scalar) and $V_\mu^{(\pm)}$ (massive vector) are left generic, with the only requirement that the interactions preserve the QED gauge symmetry and any other symmetry imposed by the new theory, if present. Interactions between a photon and new particles may also be present, and the lagrangian term will be just the same as the usual QED.

We can make a general classification of NP contributions to dipole transitions at one-loop following Refs. [3, 30, 31]. All the relevant topologies are shown in Figure 2, where we classify them as neutral scalar, Fig. 2(a), neutral vector boson, Fig. 2(b), charged scalar, Fig. 2(c), and charged vector boson, Fig. 2(d).

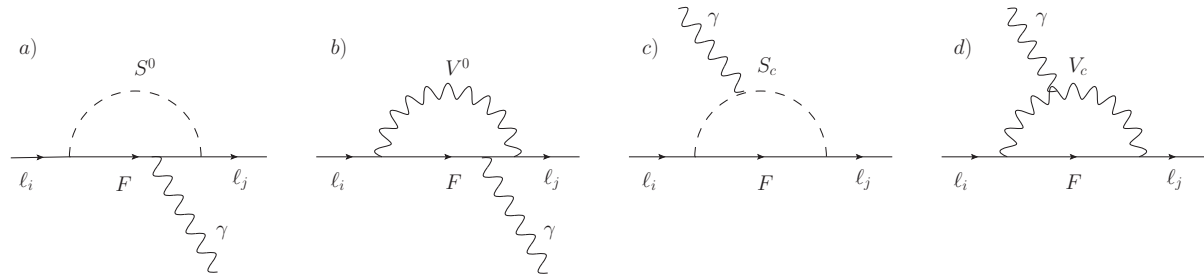


Fig. 2: New physics contributions to dipole transitions at one loop: (a) neutral scalar - charged fermion, (b) neutral vector boson - charged fermion, (c) charged scalar - neutral fermion and (d) charged vector boson - neutral fermion.

⁷The unit e cm is the dipole moment of an e^+e^- pair separated by 1 cm. The conversion factor into energy units is $\hbar c = 1.9733 \times 10^{-11}$ MeV cm.

⁸Additionally, processes such as $b \rightarrow s \gamma$ in the quark sector play also a very relevant role.

We have computed the one-loop contributions to the dipole coefficients from diagrams of Figure 2 in the unitary gauge, where the Goldstone bosons of the theory are absorbed by the massive vector bosons. For a detailed and pedagogical derivation of the dipole diagrams shown in Figure 2, computed in Feynman gauge and in the context of anomalous magnetic moments, we refer the reader to [32]. For an example involving diagrams such as Figure 2(d) in the R_ξ gauge within the context of LFV, see [33].

Since the NP particles are usually heavier than the fermions of the first and second generations, i.e. the families most interesting for phenomenology, we present the complete one loop functions for the dipole coefficients up to order $O(m_i/M_X^2)$, where M_X is the mass of the vector or scalar boson inside the loop and m_i is the mass of the external fermions. We parametrize the dipole matrix as:

$$C_{ij} = Q_F C_{ij}^{(a)} + Q_F C_{ij}^{(b)} + Q_S C_{ij}^{(c)} + Q_V C_{ij}^{(d)}, \quad (12)$$

where the contributions separately read

$$C_{ij}^{(a)} = \frac{(y_L)_{ik}(y_L)_{jk}^* m_i + (y_R)_{ik}(y_R)_{jk}^* m_j}{M_S^2} I_1(M_{F_k}^2/M_S^2) + \frac{(y_R)_{ik}(y_L)_{jk}^* M_{F_k}}{M_S^2} I_2(M_{F_k}^2/M_S^2), \quad (13)$$

$$C_{ij}^{(b)} = \frac{(g_R)_{ik}(g_R)_{jk}^* m_i + (g_L)_{ik}(g_L)_{jk}^* m_j}{M_V^2} I_3(M_{F_k}^2/M_V^2) + \frac{(g_L)_{ik}(g_R)_{jk}^* M_{F_k}}{M_V^2} I_4(M_{F_k}^2/M_V^2), \quad (14)$$

$$C_{ij}^{(c)} = \frac{(y_L)_{ik}(y_L)_{jk}^* m_i + (y_R)_{ik}(y_R)_{jk}^* m_j}{M_S^2} J_1(M_{F_k}^2/M_S^2) + \frac{(y_R)_{ik}(y_L)_{jk}^* M_{F_k}}{M_S^2} J_2(M_{F_k}^2/M_S^2), \quad (15)$$

$$C_{ij}^{(d)} = \frac{(g_R)_{ik}(g_R)_{jk}^* m_i + (g_L)_{ik}(g_L)_{jk}^* m_j}{M_V^2} J_3(M_{F_k}^2/M_V^2) + \frac{(g_L)_{ik}(g_R)_{jk}^* M_{F_k}}{M_V^2} J_4(M_{F_k}^2/M_V^2), \quad (16)$$

and Q_i are the electromagnetic charges of the particles that couple to the photon in the loop. Then, the loop functions are given by:

$$I_1(x) = \frac{1}{12(1-x)^4} [2 + 3x - 6x^2 + x^3 + 6x \log x], \quad I_2(x) = \frac{1}{2(1-x)^3} [-3 + 4x - x^2 - 2 \log x], \quad (17)$$

$$I_3(x) = \frac{1}{12(1-x)^4} [-8 + 38x - 39x^2 + 14x^3 - 5x^4 + 18x^2 \log x], \quad I_4(x) = \frac{1}{2(1-x)^3} [4 - 3x - x^3 + 6x \log x], \quad (18)$$

$$J_1(x) = \frac{1}{12(1-x)^4} [-1 + 6x - 3x^2 - 2x^3 + 6x^2 \log x], \quad J_2(x) = \frac{1}{2(1-x)^3} [-1 + x^2 - 2x \log x], \quad (19)$$

$$J_3(x) = \frac{1}{12(1-x)^4} [-10 + 43x - 78x^2 + 49x^3 - 4x^4 - 18x^3 \log x], \quad J_4(x) = \frac{1}{2(1-x)^3} [4 - 15x + 12x^2 - x^3 - 6x^2 \log x]. \quad (20)$$

The limits of these functions for $x \rightarrow 0$, that will be relevant later, are

$$I_1(x) \xrightarrow{x \rightarrow 0} \frac{1}{6}, \quad I_2(x) \xrightarrow{x \rightarrow 0} -\frac{3}{2} - \log x, \quad I_3(x) \xrightarrow{x \rightarrow 0} -\frac{2}{3}, \quad I_4(x) \xrightarrow{x \rightarrow 0} 2, \quad (21)$$

$$J_1(x) \xrightarrow{x \rightarrow 0} -\frac{1}{12}, \quad J_2(x) \xrightarrow{x \rightarrow 0} -\frac{1}{2}, \quad J_3(x) \xrightarrow{x \rightarrow 0} -\frac{5}{6}, \quad J_4(x) \xrightarrow{x \rightarrow 0} 2. \quad (22)$$

Considering the flavor diagonal coefficients, we notice that all the contributions proportional to the external fermion masses are real, and so they only contribute to the anomalous magnetic moment. Then, contribution to EDMs can stem only from the chirally enhanced term, where CP-violation is possible if the theory is chiral (i.e. left-handed SM fermions couple to the NP particles differently from the right-handed ones).

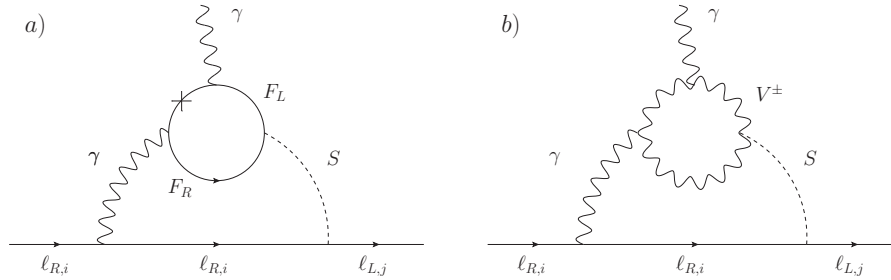


Fig. 3: Two-loop ‘‘Barr-Zee’’ diagrams contributing to the dipole transitions with a) charged fermion inner-loop or b) charged vector boson loop.

In addition, there exist two-loop diagrams, such as the famous Barr-Zee diagrams [34], that can be important when one-loop diagrams are suppressed by small couplings, as the first or second generation Yukawa couplings. In these diagrams, the suppression from the additional loop factor can be compensated by larger couplings.

Figure 3 shows two typical Barr-Zee diagrams, where a fermion or boson loop connects to the external fermion line through a (pseudo)scalar and a gauge boson. For instance, in the context of the SM, these diagrams replace one small Yukawa coupling and a light mass from the diagram in Figure 2(a) with either two gauge couplings and a larger Yukawa and mass from a heavier fermion (Figure 3(a)) or three gauge couplings (Figure 3(b)), along with an additional loop factor. In many beyond the SM theories, the main contribution comes from the diagram where the connecting gauge boson is the SM photon⁹. The Barr-Zee contribution to the dipole operator, considering only the dominant photon contribution, is [35]:

$$C_{ij}^{BZ(a)} = -\frac{2\alpha Q_F^2}{\pi M_F} (y_R)_{ij} [\text{Re}\{y_F\} f(x) + i \text{Im}\{y_F\} g(x)], \quad (23)$$

$$C_{ij}^{BZ(b)} = \frac{\alpha Q_V^2 g}{2\pi M_V} (y_R)_{ij} \left[3f(x) + \frac{23}{4}g(x) + \frac{3}{4}h(x) + \frac{f(x) - g(x)}{2x} \right], \quad (24)$$

where, $x = M_{F,V}^2/M_S^2$ and y_F is the Yukawa couplings between the scalar, S , and the internal fermion, F , defined as $y_F S \bar{F}_L F_R$. For a pure scalar particle y_R is a real number, while for a pseudoscalar it is purely imaginary. The loop functions in these expressions are given by

$$f(x) = \frac{1}{2}x \int_0^1 dz \frac{1-2z(1-z)}{z(1-z)-x} \ln \frac{z(1-z)}{x}, \quad (25)$$

$$g(x) = \frac{1}{2}x \int_0^1 dz \frac{1}{z(1-z)-x} \ln \frac{z(1-z)}{x}, \quad (26)$$

$$h(x) = \frac{1}{2}x \int_0^1 dz \frac{1}{z(1-z)-x} \left[1 + \frac{x}{x-z(1-z)} \ln \frac{z(1-z)}{x} \right]. \quad (27)$$

As we explained in the previous section, the relationship between dipole and mass operators is very relevant to limit the maximum possible enhancement of dipole operators. Indeed, detaching the external photon line from the diagrams in Figure 2 leads to a modification of the lepton mass term in the Lagrangian.

Though Lagrangian parameters are always scheme dependent and do not represent directly physical observables, the presence of radiative corrections much larger than the measured experimental values necessarily requires a sizable fine-tuning between tree-level parameters and the loop corrections. For example, if we consider the scalar loop in Figure 2(a), the finite correction to SM fermion mass at one-loop in the \overline{MS} scheme is,

$$(m_\ell^{\overline{MS}})_{ij} = m_\ell^0 \delta_{ij} - (y_R)_{ik} (y_L)_{jk}^* M_{F_k} K_1 \left(\frac{M_{F_k}^2}{M_S^2} \right), \quad (28)$$

where m_0 is the bare mass and the loop function,

$$K_1(x) = \frac{1}{16\pi^2} \left(\frac{x-1-\log x}{x-1} \right). \quad (29)$$

From this equation, we see that this expression corresponds to the second term in Eq.(13), with a slightly different loop function. Therefore, a large enhancement in the dipole operators necessarily implies a substantial one-loop correction to the fermion mass. Moreover, these one-loop corrections to the two point function may induce off-diagonal mass terms or an imaginary contribution to the fermion masses. In order to work in the mass eigenstate basis, the diagonalization and rephasing of the mass matrix must be done order by order before calculating the physical values of anomalous magnetic moments, dipole moments and lepton flavor violating transitions. This procedure can, in turn, induce new flavor or CP violating interactions.

Vector boson loops also contribute to the one-loop corrections to the mass and share the same relation to dipole observables. However, since the fermion mass is not a direct physical observable, the gauge boson contribution is generally gauge-dependent and involves the symmetry-breaking sector. Therefore, we do not discuss it further here.

The expressions presented in this section encompass most of the NP contributions at the one-loop level and highlight the intimate relation between masses and dipole operators. More exotic contributions, such as models with doubly charged fermions or scalars, can be straightforwardly obtained from this by summing the contributions of the charged fermion and charged boson with the corresponding charges.

In the following sections we will present the contributions to dipole moments from some of the most studied extensions of the SM.

3.1 Two-Higgs doublet models

Two Higgs Doublet Models (2HDMs) are the minimal extensions of the SM; they introduce a second Higgs doublet, also associated with the electroweak symmetry-breaking scale. The presence of an additional Higgs doublet is motivated by many Beyond the SM scenarios, such as Supersymmetry or Peccei-Quinn models. Moreover, models with multiple scalars allow for new sources of CP violation, both in the scalar potential and the Yukawa sector. For an extensive review on 2HDMs, we refer the reader to [36].

⁹Due to Furry's theorem, only the vector part of the Z - f - f vertex contributes, and its coupling is accidentally suppressed by a factor $(\frac{1}{4} - \sin^2\theta) \sim 0.03$ compared to the QED one.

In these models, we call Φ_1 and Φ_2 the two Higgs doublets, both carrying hypercharge $+1$ ¹⁰.

$$\Phi_a = \begin{pmatrix} \phi_a^+ \\ (v_a + \rho_a + i\sigma_a)/\sqrt{2} \end{pmatrix}. \quad (30)$$

We define also the charge-conjugate fields $\tilde{\Phi}_a \equiv i\tau_2 \Phi_a^*$ with hypercharge -1 . In general, both scalars acquire vacuum expectation values (vevs), and contribute to the total electroweak symmetry breaking $v = \sqrt{v_1^2 + v_2^2} = 246$ GeV. We define $\tan\beta = v_2/v_1$, such that the total vev can be written as $v = v_1 \cos\beta + v_2 \sin\beta$.

In general, the scalar potential includes several complex parameters which can allow scalar-pseudoscalar mixing. At this point, we neglect this possible CP violating mixing, that we will discuss at the end of the section. Then, the physical spectrum of the 2HDM, after electroweak symmetry breaking, contains a charged Higgs, H^\pm , a CP-odd Higgs, A , and two CP-even Higgs bosons, H and h , which are linear combination of ρ_1 and ρ_2 .

$$\begin{pmatrix} h \\ H \end{pmatrix} = \begin{pmatrix} -\sin\alpha & \cos\alpha \\ \cos\alpha & \sin\alpha \end{pmatrix} \begin{pmatrix} \rho_1 \\ \rho_2 \end{pmatrix}. \quad (31)$$

Similarly, the physical pseudoscalar, charged Higgs and would-be Goldstone bosons, are given by:

$$\begin{pmatrix} G^0 \\ A \end{pmatrix} = \begin{pmatrix} \cos\beta & \sin\beta \\ -\sin\beta & \cos\beta \end{pmatrix} \begin{pmatrix} \sigma_1 \\ \sigma_2 \end{pmatrix}, \quad \begin{pmatrix} G^+ \\ H^+ \end{pmatrix} = \begin{pmatrix} \cos\beta & \sin\beta \\ -\sin\beta & \cos\beta \end{pmatrix} \begin{pmatrix} \phi_1^+ \\ \phi_2^+ \end{pmatrix}, \quad (32)$$

where G^0 and G^+ are the would-be Goldstone bosons eaten by the Z and W bosons. We can also define the Higgs basis, where only one Higgs, H_1 , get a vev breaking the electroweak symmetry, that is obtained through the same rotation matrix,

$$\begin{pmatrix} H_1 \\ H_2 \end{pmatrix} = \begin{pmatrix} \cos\beta & \sin\beta \\ -\sin\beta & \cos\beta \end{pmatrix} \begin{pmatrix} \Phi_1 \\ \Phi_2 \end{pmatrix}. \quad (33)$$

The most general Yukawa Lagrangian for the leptonic sector in 2HDM is given by,

$$-\mathcal{L}_{\text{yukawa}}^{\text{2HDM}} = \bar{L}_i \ell_{R,j} Y_{ij}^{(1)} \Phi_1 + \bar{L}_i \ell_{R,j} Y_{ij}^{(2)} \Phi_2 + \text{H.c.} \quad (34)$$

Using the definitions above and in the limit of CP conservation, the interactions of the physical scalar mass eigenstates, in the basis of diagonal charged lepton masses, are,

$$\begin{aligned} -\mathcal{L}_{\text{yukawa}}^{\text{2HDM}} &= \bar{L}_{L,i} \ell_{R,j} \frac{\tilde{Y}_{ij}}{\sqrt{2}} (H \cos(\beta - \alpha) + h \sin(\beta - \alpha)) + \bar{L}_{L,i} \ell_{R,j} \frac{\rho_{ij}}{\sqrt{2}} (-H \sin(\beta - \alpha) + h \cos(\beta - \alpha)) \\ &\quad + i \bar{L}_{L,i} \ell_{R,j} \frac{\rho_{ij}}{\sqrt{2}} A + \bar{L}_{L,i} \ell_{R,j} \rho_{ij} H^+ + \text{H.c.} \\ &= \bar{L}_{L,i} \ell_{R,j} H \left(\delta_{ij} \frac{g m_i^\ell}{2 M_W} \cos(\beta - \alpha) - \frac{\rho_{ij}}{\sqrt{2}} \sin(\beta - \alpha) \right) + \bar{L}_{L,i} \ell_{R,j} h \left(\delta_{ij} \frac{g m_i^\ell}{2 M_W} \sin(\beta - \alpha) + \frac{\rho_{ij}}{\sqrt{2}} \cos(\beta - \alpha) \right) \\ &\quad + i \bar{L}_{L,i} \ell_{R,j} \frac{\rho_{ij}}{\sqrt{2}} A + \bar{L}_{L,i} \ell_{R,j} \rho_{ij} H^+ + \text{H.c.} \end{aligned} \quad (35)$$

where we defined, $\tilde{Y}_{ij} = (Y_{ij}^{(1)} \cos\beta + Y_{ij}^{(2)} \sin\beta)$, and $\rho_{ij} = (-Y_{ij}^{(1)} \sin\beta + Y_{ij}^{(2)} \cos\beta)$. We have used that \tilde{Y} is the coupling of H_1 to the leptons, and therefore, in this basis, $\tilde{Y}_{ij}/\sqrt{2} = \delta_{ij} m_i^\ell/v = \delta_{ij} g m_i^\ell/(2 M_W)$.

Nevertheless, a general 2HDM with generic ρ_{ij} couplings, as happens when both doublets couple simultaneously to the fermions, which is called Type III, has usually too large tree-level Flavour Changing Neutral Currents (FCNC). This is usually avoided imposing a Z_2 symmetry to forbid some of these Yukawa interactions, in the models with Natural Flavour Conservation (NFC). In NFC models the two Higgs doublets are distinguished by their Z_2 charge, with $\Phi_1 \rightarrow -\Phi_1$ and $\Phi_2 \rightarrow \Phi_2$. Based on the fermion transformations under Z_2 , we can distinguish different models:

- Type I 2HDM: all other SM particles are even under Z_2 , so that all fermions couple only to Φ_2 .

¹⁰Here we use the convention where the electric charge is $Q = T_3 + \frac{Y}{2}$

	Type I	Type II	Type X	Type Y
ξ_h^ℓ	$\cos\alpha/\sin\beta$	$-\sin\alpha/\cos\beta$	$-\sin\alpha/\cos\beta$	$\cos\alpha/\sin\beta$
ξ_H^ℓ	$\sin\alpha/\sin\beta$	$\cos\alpha/\cos\beta$	$\cos\alpha/\cos\beta$	$\sin\alpha/\sin\beta$
ξ_A^ℓ	$\cot\beta$	$-\tan\beta$	$-\tan\beta$	$\cot\beta$

Table 2: Mixing factors in the leptonic Yukawa interactions for natural flavor conservation 2HDM.

- Type II 2HDM: it enforces $d_{iR} \rightarrow -d_{iR}$ and $\ell_{iR} \rightarrow -\ell_{iR}$, so that Φ_1 couples only to down-quarks and charged leptons and Φ_2 to up quarks and neutrinos (if right-handed neutrinos are also present).
- Type X (or lepton-specific): all quarks are even and couple to Φ_2 , while the charged leptons are odd and couple to Φ_1 .
- Type Y model: the up-type quarks and charged leptons (even) couple to Φ_2 , while the down-type quarks (odd) to Φ_1 .

Type III models have the general scalar-fermion interactions in Eq. (35), but in models with NFC (types I, II, X and Y) the two Yukawa matrices coupling to a given fermion species can be diagonalized simultaneously and FCNCs are avoided. In these cases, the Yukawa Lagrangian is simplified,

$$\mathcal{L}_{\text{Yukawa}}^{2\text{HDM}} = -\frac{g m_i^\ell}{2 M_W} \xi_h^\ell \bar{\ell}_L \ell_R h - \frac{g m_i^\ell}{2 M_W} \xi_H^\ell \bar{\ell}_L \ell_R H - i \frac{g m_i^\ell}{2 M_W} \xi_A^\ell \bar{\ell}_L \ell_R A - \frac{g m_i^\ell}{\sqrt{2} M_W} \xi_A^\ell \bar{\nu}_L \ell_R H^+ + \text{H.c.} \quad (36)$$

The ξ_ℓ^a couplings for the four NFC versions of the 2HDM are compiled in Table 2.

Now, to obtain the contributions of 2HDM to dipole moments, we can apply the general formulas in Eqs. (12–16). The scalar couplings, $(y_L^{(a)})_i, (y_R^{(a)})_i$, of states with defined CP properties, would be,

$$\begin{aligned} (y_R^{(h)})_{ij} &= (y_L^{(h)})_{ij} = \delta_{ij} \frac{g m_i^\ell}{2 M_W} \xi_h^\ell & (y_R^{(H)})_{ij} &= (y_L^{(H)})_{ij} = \delta_{ij} \frac{g m_i^\ell}{2 M_W} \xi_H^\ell \\ (y_R^{(A)})_{ij} &= (y_L^{(A)})_{ji}^* = i \delta_{ij} \frac{g m_i^\ell}{2 M_W} \xi_A^\ell & (y_R^{(H^*)})_{ij} &= (y_L^{(H^*)})_{ij} = \delta_{ij} \frac{g m_i^\ell}{\sqrt{2} M_W} \xi_A^\ell. \end{aligned} \quad (37)$$

Thus, we see that all couplings are flavor conserving and proportional to lepton masses. So, the dipole Wilson coefficients are,

$$C_{ij} = \delta_{ij} \frac{g^2 m_i^3}{4 M_W^2} \left(\sum_{a=h,H} \frac{(\xi_a^\ell)^2}{M_a^2} (2 I_1(m_i^2/M_a^2) + I_2(m_i^2/M_a^2)) + \frac{(\xi_A^\ell)^2}{M_A^2} (2 I_1(m_i^2/M_A^2) - I_2(m_i^2/M_A^2)) + \frac{(\xi_{H^*}^\ell)^2}{M_{H^*}^2} J_1(m_i^2/M_{H^*}^2) \right). \quad (38)$$

We see that, because of the form of the scalar couplings, all contributions are necessarily proportional to m_i^3 . Therefore, to have a sizable effect, we need to compensate this suppression either with a large ξ_a^ℓ factor, or with a small scalar mass.

In Type I and type Y 2HDM, we do not expect a large enhancement from the ξ_a^ℓ couplings, as they are either $O(1)$ or proportional to $\cot\beta$, that can not be very large due to top quark Yukawa perturbativity and constraints on Higgs masses from colliders [36–38]. On the other hand in Type II and Type X, these couplings are enhanced by $\tan\beta$. In Type II or Type X, the Wilson coefficient would be,

$$C_{ij} = \delta_{ij} \frac{g^2 m_i^3}{4 M_W^2} \left(\frac{\sin^2 \alpha}{M_h^2 \cos^2 \beta} \tilde{I}(m_i^2/M_h^2) + \frac{\cos^2 \alpha}{M_H^2 \cos^2 \beta} \tilde{I}(m_i^2/M_H^2) + \frac{\tan^2 \beta}{M_A^2} \tilde{I}'(m_i^2/M_A^2) + \frac{\tan^2 \beta}{M_{H^*}^2} J_1(m_i^2/M_{H^*}^2) \right), \quad (39)$$

where we defined $\tilde{I}(x) = 2 I_1(x) + I_2(x)$ and $\tilde{I}'(x) = 2 I_1(x) - I_2(x)$. Given that the masses involved in NFC models are always the SM lepton masses, we can analyze this contribution in the limit $m_\ell/M_S \rightarrow 0$,

$$C_{ij} \simeq \delta_{ij} \frac{g^2 m_i^3}{4 M_W^2} \left(\left(\frac{\sin^2 \alpha}{M_h^2 \cos^2 \beta} + \frac{\cos^2 \alpha}{M_H^2 \cos^2 \beta} \right) \left(-\frac{7}{6} - \log \frac{m_i^2}{M_H^2} \right) + \frac{\tan^2 \beta}{M_A^2} \left(\frac{11}{6} + \log \frac{m_i^2}{M_A^2} \right) - \frac{\tan^2 \beta}{12 M_{H^*}^2} \right). \quad (40)$$

For later use, it is useful to express the Higgs mixings in terms of the angle $(\beta - \alpha)$, that parametrizes the rotation between the Higgs basis and the mass basis,

$$\begin{aligned} -\frac{\sin \alpha}{\cos \beta} &= \sin(\beta - \alpha) - \cos(\beta - \alpha) \tan \beta \\ \frac{\cos \alpha}{\cos \beta} &= \cos(\beta - \alpha) + \sin(\beta - \alpha) \tan \beta. \end{aligned} \quad (41)$$

A popular limit in 2HDM, given the absence of experimental signals of extra scalars, is the decoupling limit. The decoupling limit refers to the situation in which one of the two Higgs doublets becomes very heavy and effectively decouples from the low-energy spectrum, leaving behind a light Higgs boson that behaves like the SM Higgs. This limit corresponds to $M_H, M_A, M_{H^*} \gg v$ and $\sin(\beta - \alpha) \rightarrow 1$.

Finally, general type III 2HDM, has more freedom in the scalar couplings, although the requirement of naturalness would constrain both the $Y_{ij}^{(1)}$ and $Y_{ij}^{(2)}$ matrices to be of the order of the corresponding i or j lepton Yukawas, m_i/v or m_j/v . The scalar couplings in type III model are,

$$\begin{aligned} (y_R^{(h)})_{ij} &= (y_L^{(h)})_{ji}^* = -\delta_{ij} \frac{g m_i^\ell}{2 M_W} \sin(\beta - \alpha) - \frac{\rho_{ij}}{\sqrt{2}} \cos(\beta - \alpha) & (y_R^{(H)})_{ij} &= (y_L^{(H)})_{ji}^* = -\delta_{ij} \frac{g m_i^\ell}{2 M_W} \cos(\beta - \alpha) + \frac{\rho_{ij}}{\sqrt{2}} \sin(\beta - \alpha) \\ (y_R^{(A)})_{ij} &= (y_L^{(A)})_{ji}^* = -i \frac{\rho_{ij}}{\sqrt{2}} & (y_R^{(H^*)})_{ij} &= (y_L^{(H^*)})_{ji}^* = -\rho_{ij}. \end{aligned} \quad (42)$$

and the one-loop Wilson coefficient is,

$$C_{ij} = \delta_{ij} \frac{g^2 m_i^2}{4 M_W^2} F(m_i^2) + g \frac{\sin(2(\beta - \alpha))}{4 \sqrt{2} M_W} \left[\rho_{ij} (m_i^2 G(m_i^2) + m_j^2 G(m_j^2)) + \rho_{ji}^* m_i m_j (H(m_i^2) + H(m_j^2)) \right] +$$

$$\left(m_i \rho_{ki}^* \rho_{kj} + m_j \rho_{ik} \rho_{jk}^* \right) \left(\frac{\cos^2(\beta - \alpha)}{2 M_h^2} I_1(m_k^2/M_h^2) + \frac{\sin^2(\beta - \alpha)}{2 M_H^2} I_1(m_k^2/M_H^2) + \frac{I_1(m_k^2/M_A^2)}{2 M_A^2} + \frac{J_1(m_k^2/M_{H^\pm}^2)}{M_{H^\pm}^2} \right) +$$

$$m_k \rho_{ik} \rho_{kj} \left(\frac{\cos^2(\beta - \alpha)}{2 M_h^2} I_2(m_k^2/M_h^2) + \frac{\sin^2(\beta - \alpha)}{2 M_H^2} I_2(m_k^2/M_H^2) + \frac{I_2(m_k^2/M_A^2)}{2 M_A^2} \right), \quad (43)$$

where we defined the functions:

$$F(x^2) = \frac{\sin^2(\alpha - \beta)}{M_h^2} \tilde{I}(x^2/M_h^2) + \frac{\cos^2(\alpha - \beta)}{M_H^2} \tilde{I}(x^2/M_H^2), \quad H(x^2) = \frac{I_1(x^2/M_h^2)}{M_h^2} - \frac{I_1(x^2/M_H^2)}{M_H^2},$$

$$G(x^2) = \frac{I_1(x^2/M_h^2) + I_2(x^2/M_h^2)}{M_h^2} - \frac{I_1(x^2/M_H^2) + I_2(x^2/M_H^2)}{M_H^2}. \quad (44)$$

From this expression we see that some of the scalar couplings are not directly proportional to the masses, but that are instead replaced by the ρ_{ij} matrix. Moreover, this matrix is not necessarily diagonal in the basis of diagonal charged lepton masses. This feature may increase the 2HDM contribution in some cases, particularly in lepton flavor violating processes.

Nevertheless, since both \tilde{Y}_{ij} and ρ_{ij} are linear combinations of $Y^{(1)}$ and $Y^{(2)}$, it is clear that ρ_{ij} can not be generally $O(1)$, but both matrices should be determined by the fermion masses. This idea is captured in the Cheng-Sher ansatz [39], where $\rho_{ij} = \lambda_{ij} \sqrt{2 m_i m_j}/v$, with $\lambda_{ij} \sim O(1)$, and experimental constraints confirm this ansatz for scalar masses around the electroweak scale.

As a consequence, a double insertion of a scalar interaction in one-loop diagrams can be subdominant compared to a two-loop contribution with larger couplings, especially when the first generations are involved. This is the case of the Barr-Zee diagrams, presented in Section 2.

To understand the relevance of Barr-Zee diagrams, we can compare the diagram in Figure2(a) with Figure3 (a), which contains a top quark inside the loop. From Eq. (23), defining the scalar couplings to the top quark, $\xi_S^u g m_t P_R/(2 M_W)$ (where S denoting the scalar and P_R the right-handed projector), and in the limit of conserved CP, this contribution would be,

$$C_{ij}^t = -\frac{6\alpha Q_u^2}{\pi m_t} \frac{g m_t}{2 M_W} \left[\left(\frac{g m_t^\ell \delta_{ij}}{2 M_W} \sin(\beta - \alpha) + \frac{\rho_{ij}}{\sqrt{2}} \cos(\beta - \alpha) \right) \xi_h^u f(m_t^2/M_h^2) \right.$$

$$\left. + \left(\frac{g m_t^\ell \delta_{ij}}{2 M_W} \cos(\beta - \alpha) - \frac{\rho_{ij}}{\sqrt{2}} \sin(\beta - \alpha) \right) \xi_H^u f(m_t^2/M_H^2) - \frac{\rho_{ij}}{\sqrt{2}} \xi_A^u g(m_t^2/M_A^2) \right]. \quad (45)$$

Assuming $\ell = e$, using that $\xi_h^u = \cos \alpha / \sin \beta$, $\xi_H^u = \sin \alpha / \sin \beta$, $\xi_A^u = \cot \beta$ in all the NFC models, and neglecting $O(1)$ differences from the loop functions, the one-loop diagram would be proportional to $m_e(m_e/M_S)^2$, while the second would be proportional to $m_e(6 Q_u^2 \alpha / \pi)$. Considering the ratio $M_W/m_e \simeq 1.6 \times 10^5$, the Barr-Zee diagram dominates the one-loop contribution by a factor of roughly $1 \times 10^8 (M_S/M_W)^2$.

After discussing the CP-conserving 2HDM, we now turn to the case where CP-violating phases are present in the scalar potential. In this scenario, the CP-odd and CP-even neutral scalars mix, and the physical spectrum is described by a full 3×3 mixing matrix. It is usually enough to consider the limit of small scalar-pseudoscalar mixing. Under the assumption that the pseudoscalar has only a small mixing, ϵ , with both scalar fields, we have,

$$\begin{pmatrix} h_1 \\ h_2 \\ h_3 \end{pmatrix} = \begin{pmatrix} -\sin \alpha & \cos \alpha & -\epsilon (\cos(\beta - \alpha) + \sin(\beta - \alpha)) \\ \cos \alpha & \sin \alpha & -\epsilon (\cos(\beta - \alpha) - \sin(\beta - \alpha)) \\ \epsilon (\cos \beta - \sin \beta) & \epsilon (\cos \beta + \sin \beta) & 1 \end{pmatrix} \begin{pmatrix} \rho_1 \\ \rho_2 \\ A \end{pmatrix} + O(\epsilon^2), \quad (46)$$

where ϵ parametrizes the scalar-pseudoscalar mixing. From here, we can relate the eigenstates h_i with the states of definite CP, that would be the mass eigenstates if CP is conserved,

$$h_1 \simeq h - \epsilon (\cos(\beta - \alpha) + \sin(\beta - \alpha)) A$$

$$h_2 \simeq H - \epsilon (\cos(\beta - \alpha) - \sin(\beta - \alpha)) A$$

$$h_3 \simeq A + \epsilon (\cos(\beta - \alpha) + \sin(\beta - \alpha)) h + \epsilon (\cos(\beta - \alpha) - \sin(\beta - \alpha)) H. \quad (47)$$

The contributions to the Wilson coefficients in the presence of CP violation can be obtained from Eqs. (35,36), using these replacements to obtain the new complex scalar couplings. For instance in NFC models, we obtain,

$$\begin{aligned}
 (Y_R^{(h_1)})_{ij} &= (Y_L^{(h_1)})_{ji}^* = \delta_{ij} \frac{g m_i^\ell}{2 M_W} \left(\xi_h^\ell - i\epsilon (\cos(\beta - \alpha) + \sin(\beta - \alpha)) \xi_A^\ell \right) \\
 (Y_R^{(h_2)})_{ij} &= (Y_L^{(h_2)})_{ji}^* = \delta_{ij} \frac{g m_i^\ell}{2 M_W} \left(\xi_H^\ell - i\epsilon (\cos(\beta - \alpha) - \sin(\beta - \alpha)) \xi_A^\ell \right) \\
 (Y_R^{(h_3)})_{ij} &= (Y_L^{(h_3)})_{ji}^* = \delta_{ij} \frac{g m_i^\ell}{2 M_W} \left(i \xi_A^\ell + \epsilon (\xi_h^\ell + \xi_H^\ell) \cos(\beta - \alpha) + \epsilon (\xi_h^\ell - \xi_H^\ell) \sin(\beta - \alpha) \right) \\
 (Y_R^{(H^*)})_{ij} &= (Y_L^{(H^*)})_{ji}^* = \delta_{ij} \frac{g m_i^\ell}{\sqrt{2} M_W} \xi_A^\ell.
 \end{aligned} \tag{48}$$

The corresponding Wilson coefficients are easily obtained from, Eqs. (13, 15), by making the sum over the three neutral eigenstates with we appropriate replacements in the couplings and adding the charged Higgs.

The Barr-Zee diagrams can also play an important role in the context of flavor violation and with CP violation in the scalar potential. As shown in Eq. (46), in this case we have scalar-pseudoscalar mixing and CP violating couplings to SM fermions that can give rise to Barr-Zee contributions to EDMs of the muon or electron. We can give an expression based on the general Lagrangian in Eq. (35), including both CP and flavor mixing. In the case, of small scalar-pseudoscalar mixing, using Eq. (47), and neglecting terms $\epsilon \xi_A^\ell = \epsilon \cot \beta$, we would have,

$$\begin{aligned}
 C_{ij}^t &= -\frac{6\alpha Q_u^2}{\pi m_t} \frac{g m_t}{2 M_W} \left\{ \left(\frac{g m_i^\ell \delta_{ij}}{2 M_W} \sin(\beta - \alpha) + \frac{\rho_{ij}}{\sqrt{2}} \cos(\beta - \alpha) \right) \xi_h^\mu f(x_{t1}) \right. \\
 &\quad + \left(\frac{g m_i^\ell \delta_{ij}}{2 M_W} \cos(\beta - \alpha) - \frac{\rho_{ij}}{\sqrt{2}} \sin(\beta - \alpha) \right) \xi_H^\mu f(x_{t2}) - \frac{\rho_{ij}}{\sqrt{2}} \xi_A^\mu g(x_{t3}) \\
 &\quad + i \epsilon \frac{\rho_{ij}}{\sqrt{2}} [(\cos(\beta - \alpha) + \sin(\beta - \alpha)) \xi_h^\mu f(x_{t1}) + (\cos(\beta - \alpha) - \sin(\beta - \alpha)) \xi_H^\mu f(x_{t2}) \\
 &\quad \left. + (\cos(\beta - \alpha)(\xi_h^\mu + \xi_H^\mu) + \sin(\beta - \alpha)(\xi_h^\mu - \xi_H^\mu)) f(x_{t3}) \right] \Big\},
 \end{aligned} \tag{49}$$

where $x_{ti} = m_i^2/M_{h_i}^2$. A detailed analysis of the contributions to $\mu \rightarrow e\gamma$ and the electron EDM in the context of the 2HDM can be found in [40, 41].

3.2 Supersymmetry

A very representative example of possible NP contributing to dipole moment, is given by the Minimal Supersymmetric extension of the Standard Model (MSSM) (for a pedagogical introduction to supersymmetry see [42]). In the MSSM, any SM chiral fermion is associated to a new spin-0 complex boson, called sfermion, while the SM gauge bosons and scalar fields¹¹ are associated to new Weyl fermions, called gauginos or higgsinos, which, after electroweak symmetry breaking, mix into neutralinos, χ^0 , and charginos, χ^\pm .

In the MSSM, there are two main contributions to dipole transitions. In the first, the chargino, χ^\pm , plays the role of the internal fermion in the loop of Figure (2a), while the sneutrino, $\tilde{\nu}$ (superpartner of the neutrino), acts as the scalar. The second contribution, would correspond to Figure (2c), where the neutralino, χ^0 , is the internal fermion and the charged slepton, \tilde{l} (scalar superpartner of the lepton), is the scalar [43–45].

The internal chirality change is given by the chargino or neutralino mass, respectively, providing, at first sight, a large enhancement factor M_χ/m_t . Chargino masses are constrained to be larger than several hundreds of GeV by LEP and LHC searches, and neutralino are typically a factor two lighter. For instance, in the case of the muon, this factor leads to a 10^3 enhancement in these diagrams. However, we have to take into account the scalar couplings y_L^S and y_R^S , that can be small, as we have seen in the 2HDM, and play an important role in the overall contribution.

We start by analyzing the chargino-sneutrino diagram. Chargino eigenstates are linear combinations of the fermionic partners of the W-boson, Wino, and the charged Higgs, Higgsino. These are obtained after diagonalizing the mass matrix

$$M = \begin{pmatrix} M_2 & \sqrt{2} M_W \sin \beta \\ \sqrt{2} M_W \cos \beta & \mu \end{pmatrix}. \tag{50}$$

through two unitary matrices, U, V , as

$$U^* M V^{-1} = \text{Diag.}(M_{\chi_1^\pm}, M_{\chi_2^\pm}). \tag{51}$$

¹¹Note that the cancellation of triangle anomalies require the presence of an additional Higgs doublet, so that MSSM is a Type II Two-Higgs-Doublet Model as defined in the previous section.

Similarly, the left-handed sneutrino mass is diagonalized as,

$$R^{\bar{\nu}} M_{\bar{\nu}}^2 R^{\bar{\nu}\dagger} = \text{Diag.}(M_{\bar{\nu}_1}, M_{\bar{\nu}_2}, M_{\bar{\nu}_3}). \quad (52)$$

In the end the scalar couplings are given by,

$$(y_L^{S_0})_{ia,\alpha} = -g V_{a,1} R_{ai}^{\bar{\nu}}, \quad (y_R^{S_0})_{ia,\alpha} = Y_i U_{a,2}^* R_{ai}^{\bar{\nu}}, \quad (53)$$

where i is the lepton flavor, a labels the chargino eigenstate, α the sneutrino eigenstate and g is the $SU(2)_L$ gauge coupling. Already at this point, we see that $y_L^{S_0}$, as can be seen from the mixing $V_{a,1}$, comes from the gaugino component and is proportional to the gauge coupling, while $y_R^{S_0}$ ($U_{a,2}$ corresponds to higgsino component) involves the lepton Yukawa coupling and is therefore expected to be small.

Form here, the dominant chargino, chirality enhanced, contribution to the dipole Wilson coefficient would be,

$$C_{ij}^{\chi^\pm} = \frac{-g^2 U_{a,2} V_{a,1} R_{ai}^{\bar{\nu}*} R_{aj}^{\bar{\nu}}}{M_{\bar{\nu}}^2} \frac{m_i}{\sqrt{2} M_W \cos \beta} M_{\chi_a^\pm} I_2(M_{\chi_a^\pm}^2/M_{\bar{\nu}_a}^2). \quad (54)$$

In this equation, we have used the fact that the MSSM is a Type II Two-Higgs-Doublet Model, where H_d (and \tilde{h}_d) couples to down-type quarks and charged leptons, while H_u couples to up-type quarks and neutrinos. Then, we have,

$$Y_i = \frac{g m_i}{\sqrt{2} M_W \cos \beta}. \quad (55)$$

This coupling appears because of the Higgsino component of the Chargino, indicated by the index $b = 2$ in the $U_{a,2}$. On the other hand, the coupling to the left-handed lepton is a much larger gauge coupling, with $V_{a,1}$ corresponding to the wino component. However, it is evident that we can expect a small mixing in the chargino line, going from higgsino to wino state. This can be seen using the Mass Insertion (MI) approximation [46, 47]. Following Refs. [48, 49], we have that given a $n \times n$ hermitian matrix $A = A^0 + A^1$, with $A^0 = \text{Diag}(a_1^0, \dots, a_n^0)$ and A^1 completely off-diagonal, that is diagonalized by $\mathcal{U} \cdot A \cdot \mathcal{U}^\dagger = \text{Diag}(a_1, \dots, a_n)$, we have, at first order in A^1 :

$$\mathcal{U}_{ki}^* f(a_k) \mathcal{U}_{kj} \simeq \delta_{ij} f(a_i^0) + A_{ij}^1 \frac{f(a_i^0) - f(a_j^0)}{a_i^0 - a_j^0} \quad (56)$$

We use this formula to expand the chargino Wilson coefficients with respect to the chargino mass matrix elements. In this case we have to be careful because the chargino mass matrix is not hermitian. However due to the necessary chirality flip in the chargino line, the Wilson coefficient, C_{ij} , is a function of odd powers of M_{χ^\pm} . Then

$$\sum_{k=1}^2 U_{ki} V_{kj} m_{\chi_k^\pm} A(m_{\chi_k^\pm}^2) = \sum_{k,l,m=1}^2 U_{kl} m_{\chi_k^\pm} V_{kj} U_{mi} A(m_{\chi_m^\pm}^2) U_{ml}^* \quad (57)$$

where we introduced $\sum_l U_{kl} U_{ml}^* = \delta_{km}$. Therefore, from Eq. (50), following App B. in [49], for large $\tan \beta$ and in the limit $\mu, M_2 \gg M_W$, we find that,

$$C_{ij}^{\chi^\pm} \simeq \frac{-g^2}{M_{\bar{\nu}_a}^2} \sqrt{2} M_W M_2 \mu \sin \beta \frac{m_i}{\sqrt{2} M_W \cos \beta} R_{ai}^{\bar{\nu}*} R_{aj}^{\bar{\nu}} \frac{I_2(\mu^2/M_{\bar{\nu}_a}^2) - I_2(M_2^2/M_{\bar{\nu}_a}^2)}{\mu^2 - M_2^2}, \quad (58)$$

Thus, we see that the chiral enhancement M_{χ^\pm}/m_i is compensated by the scalar couplings, leaving only the well-known $\tan \beta$ enhancement.

We also apply the MI approximation to the sneutrino line when $i \neq j$, assuming off-diagonal elements are much smaller than diagonal ones which we take all equal to $M_{\bar{\nu}}^2$. Then, we have,

$$C_{ij}^{\chi^\pm} \simeq \frac{-g^2 m_i}{M_{\bar{\nu}}^2} M_2 \mu \tan \beta \left(\delta_{ij} \frac{I_2(\mu^2/M_{\bar{\nu}}^2) - I_2(M_2^2/M_{\bar{\nu}}^2)}{\mu^2 - M_2^2} + \frac{(M_{\bar{\nu}}^2)_{ij}}{M_{\bar{\nu}}^2} \frac{-\mu^2 I_2'(\mu^2/M_{\bar{\nu}}^2) + M_2^2 I_2'(M_2^2/M_{\bar{\nu}}^2)}{M_{\bar{\nu}}^2(\mu^2 - M_2^2)} \right), \quad (59)$$

with $I_2'(x) = dI_2(x)/dx$. We can trace this process in the MI formalism, as illustrated in Figure 4. In the figure, a right-handed lepton couples

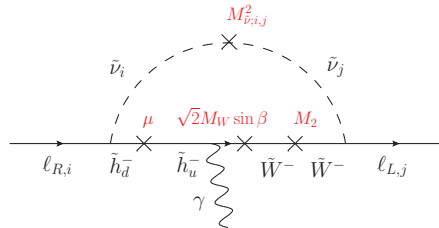


Fig. 4: Dominant chargino contribution to dipole transitions, expressed in terms of the higgsino components \tilde{h}_u , \tilde{h}_d , and wino, \tilde{W} , within the Mass Insertion Approximation. Mass insertions are denoted by crosses, with their corresponding values indicated in red.

to a left-handed sneutrino through the down-type higgsino, \tilde{h}_d^- . Along the fermion line, i) the down-type higgsino, \tilde{h}_d , converts into an up-type higgsino, \tilde{h}_u , through a μ mass term, ii) the up-type higgsino then transforms into a wino through a $\sqrt{2}M_W \sin\beta$ entry in the mass matrix, and iii) to induce a chirality flip, we need another mass insertion, leading to an odd number of insertions, which results in a wino mass, M_2 . In the sneutrino line, we can have flavour change for $i \neq j$ though an off-diagonal element in the sneutrino mass matrix, $M_{\tilde{\nu}_{i,j}}^2$. Finally, at the other end of the loop the wino couples the left handed sneutrino with a left handed lepton with a gauge (gaugino) coupling. This is the dominant, $\tan\beta$ enhanced, contribution in Eq. (59).

In a similar way, we can analyze the neutralino contribution. The couplings are now,

$$\begin{aligned} (y_L^{Sc})_{i,a,\alpha} &= \frac{g}{\sqrt{2}} \left\{ [N_{a2} + N_{a1} \tan\theta_W] R_{\alpha,i}^I - \sqrt{2} Y_i N_{a3} R_{\alpha,i+3}^I \right\}, \\ (y_R^{Sc})_{i,a,\alpha} &= -\frac{g}{\sqrt{2}} \left\{ \sqrt{2} Y_i N_{a3} R_{\alpha,i}^I + 2N_{a1} \tan\theta_W R_{\alpha,i+3}^I \right\}. \end{aligned} \quad (60)$$

In this case, the neutralino mass matrix is symmetric, and, in the basis $(\tilde{B}, \tilde{W}^0, \tilde{h}_d^0, \tilde{h}_u^0)$, is given by [42, 50],

$$M_{\chi^0} = \begin{pmatrix} M_1 & 0 & -\cos\beta s_W M_Z & \sin\beta s_W M_Z \\ 0 & M_2 & \cos\beta c_W M_Z & -\sin\beta c_W M_Z \\ -\cos\beta s_W M_Z & \cos\beta c_W M_Z & 0 & -\mu \\ \sin\beta s_W M_Z & -\sin\beta c_W M_Z & -\mu & 0 \end{pmatrix}, \quad (61)$$

with $s_W = \sin\theta_W$ and $c_W = \cos\theta_W$. This matrix is diagonalized by an orthogonal rotation, $N^* M_{\chi^0} N^\dagger = \text{Diag}(M_{\chi_1^0}, M_{\chi_2^0}, M_{\chi_3^0}, M_{\chi_4^0})$. Then, the 6×6 slepton mass matrix

$$M_{\tilde{l}}^2 = \begin{pmatrix} M_{\tilde{l}_L}^2 + (s_W^2 - \frac{1}{2})M_Z^2 \cos 2\beta & v_d (Y_{\tilde{l}}^A - Y_l \mu \tan\beta) \\ v_d (Y_{\tilde{l}}^A - Y_l \mu^* \tan\beta) & M_{\tilde{l}_R}^2 - s_W^2 M_Z^2 \cos 2\beta \end{pmatrix}, \quad (62)$$

with $M_{\tilde{l}_L}^2$, $M_{\tilde{l}_R}^2$, Y_l and $Y_{\tilde{l}}^A$ (the slepton trilinear matrix), all 3×3 matrices. This matrix is diagonalized by $R^I M_{\tilde{l}}^2 R^{I\dagger} = \text{Diag.}(M_{\tilde{l}_1}, \dots, M_{\tilde{l}_6})$.

From here, we can obtain the chirality-enhanced neutralino contribution as,

$$C_{ij}^{\chi^0} = -\frac{g^2}{2M_{\tilde{l}_a}^2} \left([N_{a2} + N_{a1} t_W] R_{\alpha,i}^I \left(2N_{a1}^* t_W R_{\alpha,j+3}^I + \frac{m_i}{M_W \cos\beta} N_{a3}^* R_{\alpha,j}^I \right) - 2 \frac{m_j}{M_W \cos\beta} N_{a1}^* N_{a3} t_W R_{\alpha,i+3}^I R_{\alpha,j+3}^I \right) M_{\chi_a^0} J_2(M_{\chi_a^0}^2/M_{\tilde{l}_a}^2), \quad (63)$$

where we neglected the Yukawa squared term.

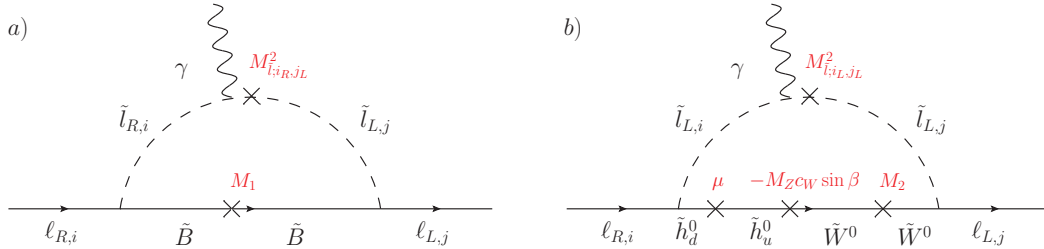


Fig. 5: Dominant neutralino contributions to dipole transitions, expressed in terms of the higgsino components \tilde{h}_u , \tilde{h}_d , bino, \tilde{B} , and wino, \tilde{W} , within the Mass Insertion Approximation. Mass insertions are denoted by crosses, with their corresponding values indicated in red. Diagram a) represents the pure bino contribution with chirality changing slepton mass insertion and b) is the mixed gaugino-higgsino contribution.

In this expression we see that we have three different terms. Once again, it is useful to apply the MI approximation to track the physics, extracting the odd neutralino mass insertion and expanding the hermitian matrix $M_{\chi^0} M_{\chi^0}^\dagger$, as we did in the chargino case. Following Ref. [49], the final expression for the dominant neutralino contribution is,

$$\begin{aligned} C_{ij}^{\chi^0} \approx & -\frac{g^2}{2} \mu \tan\beta \left(2\delta_{ij} t_W^2 \frac{m_i M_1}{M_{\tilde{l}_L}^2} \frac{M_{\tilde{l}_L}^2 J_2(M_1^2/M_{\tilde{l}_L}^2) - M_{\tilde{l}_R}^2 J_2(M_1^2/M_{\tilde{l}_L}^2)}{M_{\tilde{l}_R}^2(M_{\tilde{l}_R}^2 - M_{\tilde{l}_L}^2)} + t_W^2 \frac{m_i M_1}{M_{\tilde{l}_L}^2} \left(\delta_{ij} \frac{J_2(\mu^2/M_{\tilde{l}_L}^2) - J_2(M_1^2/M_{\tilde{l}_L}^2)}{\mu^2 - M_1^2} + \right. \right. \\ & - \frac{(M_{\tilde{l}_L}^2)_{ij}}{M_{\tilde{l}_L}^2} \frac{H(\mu^2/M_{\tilde{l}_L}^2) - H(M_1^2/M_{\tilde{l}_L}^2)}{\mu^2 - M_1^2} \left. \right) - \frac{m_i M_2}{M_{\tilde{l}_L}^2} \left(\delta_{ij} \frac{J_2(\mu^2/M_{\tilde{l}_L}^2) - J_2(M_2^2/M_{\tilde{l}_L}^2)}{\mu^2 - M_2^2} - \frac{(M_{\tilde{l}_L}^2)_{ij}}{M_{\tilde{l}_L}^2} \frac{H(\mu^2/M_{\tilde{l}_L}^2) - H(M_2^2/M_{\tilde{l}_L}^2)}{\mu^2 - M_2^2} \right) + \\ & + 2t_W \frac{m_j M_1}{M_{\tilde{l}_R}^2} \frac{(M_{\tilde{l}_R}^2)_{ij}}{M_{\tilde{l}_R}^2} \frac{H(\mu^2/M_{\tilde{l}_R}^2) - H(M_1^2/M_{\tilde{l}_R}^2)}{\mu^2 - M_1^2} \left. \right), \end{aligned} \quad (64)$$

where we introduced the function $H(x) = xJ'_2(x) + J_2(x)$ and took the limit of equal mass for all left-handed sleptons, $M_{\tilde{L}}$, and for all right-handed sleptons, $M_{\tilde{R}}$.

We can see two of these neutralino contributions in Figure 5. The first term, depicted in Figure 5a), has no apparent Yukawa suppression in the neutralino couplings and would correspond to bino exchange. Nevertheless, this term requires a left-right mixing in the slepton line from \tilde{l}_{iR} to \tilde{l}_{jL} , that from Eq. (62), in terms of mass insertions, is proportional to $\delta_{ij}^{LR} = m_i \mu \tan \beta / M_{\tilde{l}}^2$, where once more, we neglected the term not $\tan \beta$ -enhanced taking into account that trilinear couplings are $Y_i^A \sim O(\mu Y_i)$.

The second and third terms, corresponding to Figure 5b), have a higgsino coupling, proportional to the lepton Yukawa and a gaugino coupling. In the third term, we go in the fermionic line, from \tilde{h}_d to \tilde{h}_u , through a μ term, then into wino through a $\sqrt{2}M_W \sin \beta$ entry in the mass matrix, and finally we add a M_2 for a third chirality flip. On the other hand, the internal slepton is purely left-handed, with possible flavor change $i \rightarrow j$ provided by the mass insertion $(M_{\tilde{L}}^2)_{ij}/M_{\tilde{L}}^2$. The second term corresponding to bino is completely analogous.

The full supersymmetric contribution would be the sum of the the chargino and neutralino contributions and it is $\tan \beta$ enhanced

3.3 Extra $U(1)$ gauge symmetries

The addition of a new $U(1)$ gauge symmetry to the SM is one of the simplest ways to introduce new gauge interactions. The requirement of the new gauge symmetry to be anomaly-free, restricts the quantum numbers of the fermions in the theory. If we consider the SM fermion content, popular NP scenarios involve a new $U(1)$ gauge group whose fermion quantum numbers are linear combination of the baryon (B), lepton (L), and lepton flavor (L_i) numbers, such as $B - L$, $B - 3L_i$ or $L_i - L_j$.¹²

Given that most of the experimental measurements involve first-generation fermions, new gauge interactions with electrons result in either highly suppressed couplings or extremely massive boson. For this reason, we focus on new interactions involving muons and taus in the lepton sector. Following [51], we can define interaction eigenstates as follows:

$$l_{L,2} \sim (1, 2)(-1/2, q'_2), \quad l_{R,2} \sim (1, 1)(-1, q_2), \quad (65)$$

$$l_{L,3} \sim (1, 2)(-1/2, q'_3), \quad l_{R,3} \sim (1, 1)(-1, q_3), \quad (66)$$

where the quantum numbers in parenthesis correspond to the representation under $SU(3) \times SU(2) \times U(1) \times U(1)'$. Anomaly cancellation imposes the conditions $q'_2 = -q'_3$, $q_2 = -q_3$, $q'_2 = q_2$. In the following, we will always assume that the $U(1)'$ interaction is spontaneously broken, with the corresponding gauge boson acquiring a mass $M_{Z'}$. The introduction of a new abelian symmetry can induce kinetic mixing between the SM Hypercharge and the new Z' already at tree level, leading to an interaction with electrons once the gauge fields are rotated into the physical states. However, this effect can be entirely avoided at any loop order by imposing the following exact discrete symmetry:

$$\ell_{L,2} \leftrightarrow \ell_{L,3}, \quad \ell_{R,2} \leftrightarrow \ell_{R,3}, \quad B^\mu \leftrightarrow B^\mu, \quad Z'^\mu \leftrightarrow -Z'^\mu. \quad (67)$$

We will impose this symmetry for the following models; scenarios where kinetic mixing becomes relevant will be discussed later. As a first example, we consider the case where $l_{L,2} = \mu_L$, $l_{L,3} = \tau_L$, $l_{R,2} = \mu_R$, $l_{R,3} = \tau_R$, where μ_L and τ_L refers to the SM doublets. This is the case of the spontaneously broken gauged $L_\mu - L_\tau$ symmetry, a model extensively studied in the literature. The interaction Lagrangian for this model is given by,

$$\mathcal{L}_{\text{int}} = g' Z'_\alpha \left(\bar{\mu} \gamma^\alpha \mu + \bar{\nu}_\mu \gamma^\alpha P_L \nu_\mu - \bar{\tau} \gamma^\alpha \tau - \bar{\nu}_\tau \gamma^\alpha P_L \nu_\tau \right), \quad (68)$$

From the interaction Lagrangian, we obtain the couplings, $(g_R)_{ij} = (g_L)_{ij} = \delta_{ij} g' q'_i$, with $q'_1 = 0$, $q'_2 = 1$ and $q'_3 = -1$. The contributions of this model to the dipole Wilson coefficients are given by,

$$C_{ij}^{Z'(D)} = (g' q'_i)^2 \delta_{ij} \frac{m_i}{M_{Z'}^2} \left(2 I_3(m_i^2/M_{Z'}^2) + I_4(m_i^2/M_{Z'}^2) \right). \quad (69)$$

In this model, the couplings and the Wilson coefficient are flavor-diagonal, and we can only expect contributions to flavor-diagonal dipole moments that scale with the mass of the external state. However, the anomaly-free condition allows for models with flavor-changing couplings, which could induce additional enhancement in dipole transitions. This occurs if the interaction eigenstates do not coincide with the mass eigenstates. In our case, a simple example is obtained if we assign charge $q'_2 = 1$ to the fields $\ell_{L,2} = (\mu_L + \tau_L)/\sqrt{2}$ and $\ell_{R,2} = (\mu_R + \tau_R)/\sqrt{2}$ and $q'_3 = -1$ to $\ell_{L,3} = (\mu_L - \tau_L)/\sqrt{2}$ and $\ell_{R,3} = (\mu_R - \tau_R)/\sqrt{2}$ [51, 52]. The interaction Lagrangian in this case is,

$$\mathcal{L}_{\text{int}} = g' Z'_\alpha \left(\bar{\mu} \gamma^\alpha \tau + \bar{\nu}_\mu \gamma^\alpha P_L \nu_\tau + \bar{\tau} \gamma^\alpha \mu + \bar{\nu}_\tau \gamma^\alpha P_L \nu_\mu \right), \quad (70)$$

so that the couplings are now, $(g_R)_{ii} = (g_L)_{ii} = (g_R)_{1i} = (g_L)_{1i} = (g_R)_{i1} = (g_L)_{i1} = 0$ and $(g_R)_{23} = (g_R)_{32} = (g_L)_{23} = (g_L)_{32} = g'$, and the corresponding Wilson coefficients,

$$C_{22}^{Z'(FC)} = (g')^2 \frac{m_\mu}{M_{Z'}^2} \left(2 I_3(m_\tau^2/M_{Z'}^2) + \frac{m_\tau}{m_\mu} I_4(m_\tau^2/M_{Z'}^2) \right), \quad (71)$$

with off-diagonal Wilson coefficients being zero and, while the diagonal coefficient C_{33} is non vanishing, it is irrelevant, as the internal chirality change would be proportional to the muon mass. More general charge assignments are also possible and would have both flavor diagonal and flavor off-diagonal couplings even involving the first generation. For example, in the $U(1)_{L_\mu - L_\tau}$ model, we could get general

¹²Anomaly-free conditions may require the inclusion of right-handed neutrinos in the theory, especially when a linear combination of B and $L_{(i)}$ is involved.

Z' couplings if the lepton mass eigenstates are not interaction eigenstates. This can be obtained in the presence of a doublet scalar field ϕ with charge +1 under the new symmetry, with a vev contributing to the lepton mass matrix in the (1, 2) and (1, 3) entries. In this case, the rotation to the mass basis introduces off-diagonal couplings $g' Z'_a U_{ij}^{L,R} \bar{f}_{L,R}^\alpha \gamma^\alpha f_{L,R}^j$. Then, the dipole coefficients would read:

$$C_{ij} = -(g')^2 \sum_{k=2,3} \left[\frac{(U^R)_{ik}(U^R)_{jk}^* m_i + (U^L)_{ik}(U^L)_{jk}^* m_j}{M_{Z'}^2} I_3(m_k^2/M_{Z'}^2) + \frac{(U^L)_{ik}(U^R)_{jk}^* m_k}{M_{Z'}^2} I_4(m_k^2/M_{Z'}^2) \right] \quad (72)$$

This model could contribute both to flavor conserving and flavor violating observables. In the presence of physical phases, an EDM could also be generated, if left-handed couplings differ from the right-handed ones.

So far, we have considered the addition of new abelian symmetries based on the arguments of anomaly cancellation, assuming that the SM fermions are charged under the new symmetry. Nonetheless, many models in the literature consider the presence of an additional $U(1)$ dark gauge group, under which the SM particles remain uncharged. This can be employed to generate a portal through kinetic mixing with the SM hypercharge via the Lagrangian term

$$\frac{\epsilon}{2} B^{\mu\nu} Z'_{\mu\nu}. \quad (73)$$

If this additional force is long-range, meaning the gauge boson remains massless, the dark boson does not interact with SM fermions, and therefore, this interaction does not contribute to dipole operators at (one-)loop level. However, if a dark boson mass term is present, the mixing with the photon and the Z boson induces interactions with SM fermions, which are parametrized by the following Lagrangian terms:

$$\mathcal{L}_{\text{int}} \supset e Z'_\mu \epsilon \left(\cos \theta_W J_{em}^\mu + \sin \theta_W \tan \xi J_Z^\mu \right) \quad (74)$$

where $\tan \xi \equiv M_{Z'}^2 / (M_Z^2 - M_{Z'}^2)$ and the Z current is defined as $J_Z^\mu \equiv (J_3^\mu - \sin^2 \theta_W J_{em}^\mu) / \cos \theta_W$, with J_3^μ being the current associated with the T_3 generator of $S U(2)_L$. This results in the following contributions to the vector couplings:

$$(g_L)_{ij} = \delta_{ij} \frac{e}{2} \epsilon \left(\frac{2 \cos^2 \theta_W Q_\ell^j - (1 + 2 \sin^2 \theta_W Q_\ell^j) \tan \xi}{\cos \theta_W} \right); \quad (g_R)_{ij} = \delta_{ij} e \epsilon \left(\frac{\cos^2 \theta_W Q_\ell^j - \sin^2 \theta_W Q_\ell^j \tan \xi}{\cos \theta_W} \right). \quad (75)$$

The contribution to the dipole coefficients can be easily obtained from Eq. (14). Given the fact that this interaction is flavor conserving and real, the dark gauge boson can only contribute to real part of flavor-diagonal coefficient of dipoles.

3.4 Standard Model Effective Field Theory

Up to this point, we analyzed NP effects on dipole operators in several specific models. However, if NP is significantly heavier than the electroweak scale, we can integrate out the heavy degrees of freedom to get a tower of higher dimensional operators and treat the SM as an effective field theory (SMEFT). In fact, this is typically needed in most of the theories mentioned in the previous sections to apply the Renormalization Group Evolution (RGE) of the different operators and calculate the observables at energy scales of the order of the lepton masses. From another perspective, since no NP has been discovered up to the TeV scale, parameterizing short-distance effects using the SMEFT framework turns out to be a powerful tool for making predictions without relying on a specific ultraviolet (UV) theory. The SMEFT Lagrangian is parametrized as a tower of d -dimensional operators, $O_i^{(d)}$, that are invariant under the SM gauge group:

$$\mathcal{L}_{\text{SMEFT}} = \mathcal{L}_{\text{SM}} + \sum_d \sum_i \frac{C_i^{(d)}}{\Lambda^{d-4}} O_i^{(d)}, \quad (76)$$

where $C_i^{(d)}$ are the corresponding Wilson coefficients and Λ the ultraviolet cut-off of the effective theory. The SMEFT Lagrangian contains, in principle, an infinite number of operators, whose relevance diminish progressively as d increases. In this review, we focus on the operators that are usually the most relevant, those at dimension six, in the Warsaw basis [53]¹³. Among them, focusing on the lepton sector, only two types of operators can have a tensor current with gauge fields at dimension six, the electroweak dipoles:

$$O_{eB}^{ij} = \bar{l}_L \sigma_{\mu\nu} e_R^j H B^{\mu\nu}, \quad O_{eW}^{ij} = \bar{l}_L \sigma_{\mu\nu} \tau^a e_R^j H W_a^{\mu\nu}, \quad (77)$$

where $B^{\mu\nu}$ and $W_a^{\mu\nu}$ are the Hypercharge and Weak bosons field strength tensors, respectively. After electroweak symmetry breaking, these operators can be easily matched onto the dimension 5 dipoles in the broken theory,

$$C_{ij} = \frac{8\pi^2}{e} \frac{v}{\sqrt{2} \Lambda^2} (\cos \theta_W C_{eB}^{ij} - \sin \theta_W C_{eW}^{ij}). \quad (78)$$

As mentioned above, one of the key roles of SMEFT analysis is the running under RGE, which allows the resummation of large logarithms, and can have a significant impact anytime a sizable coupling or a large separation scale is involved. Furthermore, the RGE can induce mixing between different operators, allowing dimension-six operators that are not dipole operators at the UV scale to contribute to dipole-related observables at the low scales of the experiments.

¹³There is only one possible type of operator at dimension five, the Weinberg operator, which is responsible for the Majorana neutrinos mass.

All of these effects are encoded in the β function of the Wilson coefficients, which is ruled by the anomalous dimension matrix γ_{ij} , according to,

$$16\pi^2 \frac{dC_i(\mu)}{d\ln\mu} = \gamma_{ji}^{(m)} C_j(\mu), \quad (79)$$

where m labels the loop order and μ is the energy scale of the running. Diagonal elements in γ_{ij} of Eq. (79), will be responsible for the self-running, which can be sizable if the QCD gauge coupling is involved, while off-diagonal elements mix different operators in the evolution to low energies.

one-loop RGEs: LO		one-loop RGEs: NLO	
$O_{lequ(3)}^{ijlm}$	$\bar{l}_{L,i}^\alpha \sigma_{\mu\nu} e_{R,j} \epsilon_{\alpha\beta} \bar{q}_{L,l}^\beta \sigma_{\mu\nu} u_{R,m}$	$O_{lequ(1)}^{ijlm}$	$\bar{l}_{L,i}^\alpha e_{R,j} \epsilon_{\alpha\beta} \bar{q}_{L,l}^\beta u_{R,m}$
O_{HW}	$H^\dagger H W_{\mu\nu}^a W_a^{\mu\nu}$	O_{eB}^{ij}	$\bar{l}_L \sigma_{\mu\nu} e_R^j H F^{\mu\nu}$
$O_{H\bar{W}}$	$H^\dagger H \bar{W}_{\mu\nu}^a W_a^{\mu\nu}$	O_{eW}^{ij}	$\bar{l}_L \sigma_{\mu\nu} \tau^a e_R^j H W_a^{\mu\nu}$
O_{HWB}	$H^\dagger \tau^a H W_{\mu\nu}^a B_{\mu\nu}$	O_{uB}^{ij}	$\bar{l}_L \sigma_{\mu\nu} u_R^j \tilde{H} F^{\mu\nu}$
$O_{H\bar{W}B}$	$H^\dagger \tau^a H \bar{W}_{\mu\nu}^a B_{\mu\nu}$	O_{uW}^{ij}	$\bar{l}_L \sigma_{\mu\nu} \tau^a u_R^j \tilde{H} W_a^{\mu\nu}$
O_{HB}	$H^\dagger H B_{\mu\nu} B^{\mu\nu}$	O_{dB}^{ij}	$\bar{l}_L \sigma_{\mu\nu} d_R^j H F^{\mu\nu}$
$O_{H\bar{B}}$	$H^\dagger H \bar{B}_{\mu\nu} B^{\mu\nu}$	O_{dW}^{ij}	$\bar{l}_L \sigma_{\mu\nu} \tau^a d_R^j H W_a^{\mu\nu}$
		O_W	$\epsilon^{IJK} W_\mu^{I\nu} W_\nu^{J\rho} W_\rho^{K\mu}$
		$O_{\bar{W}}$	$\epsilon^{IJK} W_\mu^{I\nu} W_\nu^{J\rho} \bar{W}_\rho^{K\mu}$

(a)

(b)

Table 3: List of operators that mix to the electroweak dipoles at LO and NLO. We define $\tilde{V}^{\mu\nu} = \frac{e^{\mu\nu\rho\sigma}}{2} V_{\rho\sigma}$, where V refers to either B or W , and $\epsilon_{\alpha\beta}$ as the Levi-Civita tensor of $SU(2)$. Operators such as O_{eV} can induce mixing between dipole operators with different lepton families.

Considering a complete basis for the SMEFT lagrangian, it is possible to identify all the operators at dimension six that contribute to the dipole coefficients under RGE. Neglecting the self-running contribution, the β functions at one-loop for the Wilson coefficients of the electroweak dipoles are [54, 55]:

$$16\pi^2 \frac{dC_{eW}^{ij}}{d\ln\mu} = -2g_2 N_c C_{lequ(3)}^{ijlm} [Y_u]_{ml} - [Y_e^\dagger]_{ij} \left(g_2 (C_{HW} + iC_{H\bar{W}}) + g_1 (y_l + y_e) (C_{HWB} + iC_{H\bar{W}B}) \right) \quad (80)$$

$$16\pi^2 \frac{dC_{eB}^{ij}}{d\ln\mu} = 4g_1 N_c (y_u + y_q) C_{lequ(3)}^{ijlm} [Y_u]_{ml} - [Y_e^\dagger]_{ij} \left(2g_1 (y_l + y_e) (C_{HB} + iC_{H\bar{B}}) + \frac{3}{2} g_2 (C_{HWB} + iC_{H\bar{W}B}) \right), \quad (81)$$

where $g_{1,2}$ are the hypercharge and weak gauge couplings, $Y_{u,e}$ are the up quark and lepton Yukawa matrices and y_i are the SM hypercharges. The indices i, j, l, m label the fermion flavors. The different operators associated to the Wilson coefficients in Eq. (80,81) are shown in Table (3a).

From these operators, some of them, such as $O_{HV(V)}$ and $O_{H\bar{V}(V)}$ are Hermitian, requiring their Wilson coefficients to be real. In particular, $O_{HV(V)}$ is CP-even, while $O_{H\bar{V}(V)}$ is CP odd, so that they contribute to the anomalous magnetic moments and EDMs, respectively. Looking at Eqs. (80, 81), LFV in dipole observables through these latter operators could only be triggered by the lepton Yukawa matrix. However, in the SM, Y_e is real and diagonal, so that processes such as $\ell_i \rightarrow \ell_j \gamma$ cannot be induced by these operators at dimension six. Effects induced by a modification of the Yukawa texture are discussed below.

In contrast, the operator $O_{lequ(3)}$ is not hermitian and allows transitions between different families. As a result, it can affect all the dipole observables, if sources of CP and flavor violation are present in the UV completion of the model. Additionally, the correspondent anomalous dimension is proportional to the up quark Yukawa matrix, so that a large enhancement can occur when top quarks are present in the loop. This operator is particularly interesting because it is generated by integrating out heavy scalars that couple to quarks and leptons in the same interaction, usually referred to as scalar leptoquarks. These particles are predicted by Grand Unified Theory and, in the recent years, have gained popularity as candidates for the explanation of *flavor anomalies* in specific semi-leptonic B meson decays [56]¹⁴. For instance, this

¹⁴As of today, some of these *flavor anomalies* have disappeared due to a recast of the experimental data by the LHCb collaboration. However, some tensions persist when performing a global fit with other experimental measurements. See [57] for a recent review.

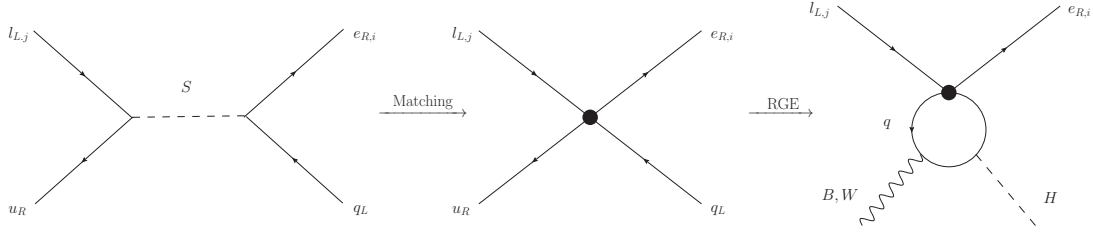


Fig. 6: Contribution from a scalar leptoquark to dipole operators, induced via the effective operator $O_{lequ(3)}$ after tree-level matching. The dipole is then generated at one-loop through renormalization group evolution (RGE).

operator is generated by a heavy scalar leptoquark with SM quantum numbers $(3, 2, 7/6)$, with interactions

$$\mathcal{L}_{Lq} \supset -y_{ij}^{qe} S \bar{q}_L^i e_R^j - y_{ij}^{lq} \tilde{S} \bar{l}_L^i u_R^j + \text{H.c.}, \quad (82)$$

with $\tilde{S} = i\tau_2 S^*$, as shown in Figure 6. If we integrate out the heavy scalar field at tree level by using the equation of motion, the resulting dimension six operator would be, $\bar{l}_{L,i} u_{R,m} \epsilon_{\alpha\beta} \bar{q}_{L,i}^\beta e_{R,j}^\alpha$, that is transformed into $O_{lequ(3)}$ after using Fiertz identities¹⁵. According to Eqs. (80, 81), this operator contributes to the dipoles at one-loop level in the RGE by closing the quark loop and attaching one Higgs boson and a B or W gauge field.

In addition, RGE resummation captures effects beyond the leading log in the one-loop β function. These arise from operators that mix with those in Eqs.(80,81) and subsequently feed into the dipole. While suppressed by extra loop factors, large logarithms or unsuppressed SM couplings can result in sizable contributions to dipole observables. A complete list of such operators contributing to dipole Wilson coefficients at NLO is given in Table (3b). First-generation dipole observables can be particularly sensitive to scalar four-fermion operators like $O_{lequ(1)}^{ijlm}$ or dipole-type operators O_{uV}^{ij} when top quarks are involved, due to the sizable top Yukawa coupling in the RGE.

Effects induced by finite mixing, namely operators that enter dipoles not in the RGE, are usually renormalization scheme or basis dependent, given the fact that trace of γ_5 and contribution of evanescent operators affect the finite part of the one-loop computation in an ambiguous way. In view of preserving the model independence of the SMEFT analysis, these effects can be taken under control when the two-loop anomalous dimension matrix is considered [58]. For an analysis of the two-loop effects in dipole operators see [59].

As anticipated, relevant dimension six effects can also be triggered by the modification of the Yukawa texture. Within the SMEFT, this is ruled by operators like $O_{f\varphi}^{ij} = H^\dagger H \bar{f}_i^{(\dagger)} H f_j$. Indeed, after the electroweak spontaneous symmetry breaking, they modify the SM Yukawa matrices, which are no longer proportional to the fermion mass matrix. As a result, if $C_{f\varphi}^{ij}$ is complex or off-diagonal, CP or flavour violating interactions with the Higgs and the SM fermions may survive even after rotating the fields in their mass eigenstate basis. As a consequence, this can induce observable effects in EDMs or dipole transition.

Large effects due to modified Yukawa couplings can stem from the Barr-Zee diagrams in Figure 3, with the Higgs boson as the internal scalar. Indeed, in the SM, such contributions are real and flavor diagonal so that they can impact only the anomalous magnetic moment. However, if the NP effects encoded in $O_{e\varphi}$ are not proportional to the SM Yukawa itself, these diagrams feel the modified Higgs interactions in the external lepton line, leading to possible large contribution to EDMs or $\ell_i \rightarrow \ell_j \gamma$.

4 Dipole observables

In the previous section, we derived the general expression for the “dipole matrix” at one loop and discussed additional two-loop contributions that could be relevant. Here, we apply these expressions to the main dipole observables, anomalous magnetic moments, EDMs and LFV processes, and analyze their sensitivity to physics beyond the SM.

4.1 Muon Anomalous Magnetic Moment

As explained in Section 2, among all magnetic moments, the muon magnetic moment is generally the most sensitive probe for NP. For a long-time there was a sizable discrepancy between the experimental results and SM predictions that was considered a potential sign of NP. Indeed, the uncertainty in the computation of a_μ is dominated by the Hadronic Vacuum Polarization (HVP) contribution, which corresponds to the Schwinger’s diagram with the photon propagator dressed with a hadronic bubble. Due to the fact that the QCD coupling constant becomes large at low energy, this contribution can not be reliably computed in perturbation theory. For many years, this quantity has been extrapolated from the low-energy $e^+e^- \rightarrow \text{had.}$ data, with the so-called data-driven approach. After the result of the Muon g-2 collaboration and the combination with BNL results, the discrepancy with this SM prediction is [60]:

$$\Delta a_\mu^{\text{exp}} \equiv a_\mu^{\text{exp}} - a_\mu^{\text{SM}} = (2.49 \pm 0.48) \times 10^{-9}, \quad (83)$$

¹⁵Fierz identities are algebraic relations used to rearrange products of gamma matrices and spinors, often applied in SMEFT to rewrite fermion bilinears. Caution is needed in loop calculations, as these identities hold strictly in 4D and may introduce evanescent operators when using dimensional regularization.

which correspond to a discrepancy of 5.2σ . For this reason, there is extensive literature exploring possible NP explanations for this discrepancy. Recently, a new lattice determination of the HVP by the BMW collaboration has reduced this discrepancy to the 0.9σ -level [16]. Here, we will discuss the different possibilities in general terms and refer to the comprehensive review articles for a more detailed description of specific models. Before discussing the different NP models, it is instructive to compare the size of this possible discrepancy with the weak contribution of the SM, which reads [61, 62]:

$$a_\mu^{\text{EW}}(1 \text{ loop}) \simeq \frac{G_F m_\mu^2}{12 \sqrt{2} \pi^2} [3 - 4 \sin^2 \theta_W + 8 \sin^4 \theta_W] \simeq \frac{G_F m_\mu^2}{12 \sqrt{2} \pi^2} \frac{5}{2} = 1.95 \times 10^{-9}. \quad (84)$$

This means that, with couplings of order of the gauge electroweak couplings and a chirality flip of order of the muon mass, the NP masses should be of the order of M_W to explain this discrepancy. In terms of the dipole Wilson coefficient, the electroweak contribution is,

$$C_{\mu\mu}^{\text{EW}} = \frac{5}{2} \frac{g^2}{48} \frac{m_\mu}{M_W^2} \simeq \frac{g^2}{20} \frac{m_\mu}{M_W^2}. \quad (85)$$

If we consider the new lattice computation, which agrees with the experimental measurements, the sensitivity to NP is roughly given by the errors in this difference, that if combined quadratically, would give us, $\delta a_\mu^{\text{BMW}} \simeq 0.45 \times 10^{-9}$, still of the order of the EW contribution. Given the current uncertainty in the theoretical prediction, the muon g-2 anomaly can be interpreted either as evidence for NP (when considering the data-driven result) or as a sensitivity to heavy NP (when considering the lattice-based result).

From here, we will use the electroweak contributions to determine the sensitivity of the muon anomalous magnetic moment to heavy scales of NP. As an example, we can analyze the contribution of the Type X 2HDM in the decoupling limit, $\cos(\beta - \alpha) \rightarrow 0$, and for large $\tan \beta$,

$$C_{\mu\mu}^{2\text{HDM}} \simeq \frac{g^2 m_\mu^3}{4 M_W^2} \tan^2 \beta \left(\frac{1}{M_H^2} \left(-\frac{7}{6} - \log \frac{m_\mu^2}{M_H^2} \right) + \frac{1}{M_A^2} \left(\frac{11}{6} + \log \frac{m_\mu^2}{M_A^2} \right) - \frac{1}{12 M_{H^\pm}^2} \right), \quad (86)$$

which, in the limit $M_H \simeq M_{H^\pm} \simeq M_A$ reduces to,

$$C_{\mu\mu}^{2\text{HDM}} \simeq \frac{g^2 m_\mu^3}{4 M_W^2} \frac{\tan^2 \beta}{2 M_A^2}. \quad (87)$$

For M_A larger than M_W , as we expect in the decoupling limit, we have that this contribution is suppressed by a factor $5 m_\mu^2 \tan^2 \beta / (2 M_A^2) \simeq 4.3 \times 10^{-6} \tan^2 \beta M_W^2 / M_A^2$, and therefore it is negligible. The situation regarding the muon mass suppression is the same in the non-decoupling limit, $\sin(\beta - \alpha) \rightarrow 0$, although in this case, scalars can be lighter than M_W , and, as explained in Ref. [63], could give a sizable contributions to $(g - 2)_\mu$ for a scalar mass ~ 10 GeV and $\tan \beta \sim 10$.

Even in the Type III 2HDM, the largest contribution, using the Chang-Sher ansatz and with an internal τ lepton, would be,

$$\begin{aligned} C_{\mu\mu}^{2\text{HDM}_{\text{III}}} &\simeq \frac{g^2 m_\mu m_\tau^2}{2 M_W^2} \lambda_{23} \lambda_{32} \left(\frac{\cos^2(\beta - \alpha)}{M_h^2} \left(-\frac{3}{2} - \log \frac{m_\tau^2}{M_h^2} \right) + \frac{\sin^2(\beta - \alpha)}{M_H^2} \left(-\frac{3}{2} - \log \frac{m_\tau^2}{M_H^2} \right) - \frac{1}{M_A^2} \left(-\frac{3}{2} - \log \frac{m_\tau^2}{M_A^2} \right) \right) \\ &= \frac{g^2 m_\mu m_\tau^2}{2 M_W^2} \lambda_{23} \lambda_{32} \left[\left(-\frac{3}{2} - \log \frac{m_\tau^2}{M_h^2} \right) \left(\frac{\cos^2(\beta - \alpha)}{M_h^2} + \frac{\sin^2(\beta - \alpha)}{M_H^2} - \frac{1}{M_A^2} \right) - \frac{\sin^2(\beta - \alpha)}{M_H^2} \log \frac{M_h^2}{M_H^2} + \frac{1}{M_A^2} \log \frac{M_h^2}{M_A^2} \right]. \end{aligned} \quad (88)$$

We can make a simple estimate defining an effective mass $1/\tilde{M}_H^2 = (\cos^2(\beta - \alpha)/M_h^2 + \sin^2(\beta - \alpha)/M_H^2 - 1/M_A^2)$ and neglecting the "smaller" logarithms, $\log M_h^2/M_{H,A}^2$,

$$C_{\mu\mu}^{2\text{HDM}} \simeq -\frac{g^2 m_\mu m_\tau^2}{2 M_W^2} \lambda_{23} \lambda_{32} \frac{7}{\tilde{M}_H^2}. \quad (89)$$

where we replaced, $(-3/2 - \log(m_\tau^2/M_h^2)) \simeq 7$. Comparing with the EW contribution, Eq. (85), we see that the type III is suppressed by a factor, $\simeq 0.032 \lambda_{23} \lambda_{32} M_W^2 / \tilde{M}_H^2$. Again, this contribution is too small for scalar masses above the EW scale.

Obviously the smallness of 2HDM contribution is due to the proportionality of Yukawa couplings to the fermion masses. In this situation, in spite of being a two-loop contribution, the Barr-Zee diagram can be relevant. From Eq. (45), assuming that $\rho_{22} \sim m_\mu/v$, and defining an effective loop function, $\tilde{f}(m_t^2/M_S^2) \sim O(1)$, from the rest of the factors in this equation to make a rough estimate, we have,

$$C_{\mu\mu}^t = -\frac{6 \alpha Q_u^2}{\pi m_t} \frac{g^2 m_t m_\mu}{4 M_W^2} \tilde{f}(m_t^2/M_S^2). \quad (90)$$

Comparing this result with the EW contribution, we see that $C_{\mu\mu}^t / C_{\mu\mu}^{\text{EW}} \simeq 120 \alpha / (9\pi) \tilde{f}(m_t^2/M_S^2) \simeq 0.03 \tilde{f}(m_t^2/M_S^2)$, i.e. although relatively small, it is indeed larger than other 2HDM contributions.

The situation can be different in other theories like supersymmetry, where some of this scalar couplings are related to gauge couplings. Using the chargino contribution,

$$C_{\mu\mu}^{\chi^\pm} \simeq \frac{-g^2 m_\mu}{M_{\tilde{\nu}}^2} \mu M_2 \tan \beta \frac{I_2(\mu^2/M_{\tilde{\nu}}^2) - I_2(M_2^2/M_{\tilde{\nu}}^2)}{\mu^2 - M_2^2}. \quad (91)$$

We can make a simple estimate taking $\mu \simeq M_2 \simeq M_{\tilde{\nu}}$ and using $I_2(x) \xrightarrow{x \rightarrow 1} -1/4$. Then, we have,

$$C_{\mu\mu}^{\chi^\pm} \simeq \frac{g^2 m_\mu}{M_{\tilde{\nu}}^2} \frac{\tan\beta}{4}. \quad (92)$$

If we compare with the electroweak contribution, we can see that $C_{\mu\mu}^{\chi^\pm} \simeq C_{\mu\mu}^{\text{EW}}$ for $M_{\tilde{\nu}} \simeq \sqrt{5 \tan\beta} M_W$, i.e. the muon anomalous magnetic moment can be sensitive to $M_{\tilde{\nu}} \simeq 1$ TeV for $\tan\beta = 50$. From Eq. (64), we can also check that the neutralino contribution is of the same order.

The contributions to anomalous magnetic moment from extra $U(1)$ symmetries with flavor diagonal couplings, given in Eq. (69) are analogous to the electroweak contribution. Assigning charges ± 1 to the second and third generation leptons, and for small $m_\mu^2/M_{Z'}^2$, we obtain¹⁶, $C_{\mu\mu}^{Z'(D)}/C_{\mu\mu}^{\text{EW}} \simeq 13 (g'/g)^2 (M_W/M_{Z'})^2$. We can see that this contribution receives no significant enhancement, and, as expected, it is of the same order as the electroweak contribution. This implies that for Z' couplings of electroweak size, a_μ would be sensitive to Z' masses around $M_{Z'} \lesssim 300$ GeV. In Z' models with flavor-changing coupling, the contribution to the muon anomalous magnetic moment, as given in Eq (71), can receive important enhancements, proportional to the tau mass. Then, we have, $C_{\mu\mu}^{Z'(FC)}/C_{\mu\mu}^{\text{EW}} \simeq 40 m_\tau/m_\mu (g'/g)^2 (M_W/M_{Z'})^2$, and, in this case, for similar size couplings we are sensitive to masses, $M_{Z'} \lesssim 2$ TeV (for a complete analysis, taking into account other constraints in the model, see Refs. [51, 52]).

The same analysis can be repeated in any SM extension, modifying appropriately couplings and masses. For instance, we can check the contributions from a scalar leptoquark [64–66]. The enhancement in minimal models is provided by the top quark mass, and we would have, $C_{\mu\mu}^{\text{LQ}}/C_{\mu\mu}^{\text{EW}} \sim m_t/m_\mu \lambda_L \lambda_R / g^2 (M_W/M_{\text{LQ}})^2$, with $\lambda_{L,R}$ the leptoquark couplings. From here, assuming couplings of order g , the muon anomalous magnetic moment would be sensitive to scalar leptoquark masses as large as $M_{\text{LQ}} \lesssim 3.3$ TeV. However, in this case, we can not forget the contribution to the muon mass itself [67]. From Eq. (28), we would have a correction to the mass, $\Delta m_\mu/m_\mu \simeq m_t/m_\mu y_L y_R / (16\pi^2) \simeq 0.46$, for electroweak size couplings, $\lambda_L \simeq \lambda_R \simeq g$.

Finally, the sensitivity of the anomalous magnetic moment to NP can be studied in a model-independent way using the SMEFT framework. Since the same SMEFT dipole operators contribute to all the dipole observables discussed in this review, the results are largely analogous across them. The SMEFT parametrization provides a general and model-independent estimate of the energy scale to which Δa_μ is sensitive. Taking the electroweak contribution as a reference and using Eqs.(5, 78), we estimate:

$$\frac{\text{Re}[C_{eB}^{22}], \text{Re}[C_{eW}^{22}]}{\Lambda^2} \sim 10^{-5} \text{ TeV}^{-2} \quad (93)$$

Running and mixing effects depend on the matching scale to the UV theory and the energy range of the RGE evolution, making it difficult to provide a fully general result. However, in the multi-TeV regime, Ref.[62] shows that Δa_μ is primarily sensitive to the tensor operator $C_{lequ(3)}$ involving the top and charm quarks, in addition to the SMEFT dipole operators themselves.

4.2 Electric Dipole Moments

Electric dipole moments (EDMs) of the electron, neutron, or nuclei are highly suppressed in the SM due to its limited sources of CP violation. However, according to Sakharov condition, CP-violation is one of the key ingredients required to explain the observed dominance of matter over anti-matter in the universe, through a mechanism known as baryogenesis [68]. It is well known that the amount of CP-violation in the SM it is not enough for a successful baryogenesis [69, 70], requiring the presence of new sources of CP-violation coming from theory beyond the SM. For this reason, extensions of the SM typically introduce additional sources of CP violation, making EDMs highly promising probes for NP.

From Eq. (4), we have that EDMs are given by $d_\ell = -e/(4\pi^2) \text{Im}(C_{\ell\ell})$. Therefore we need the diagonal $C_{\ell\ell}$ Wilson coefficient to have an imaginary part, in the basis where charged lepton masses are real and diagonal. From Eqs. (13–16), we can see that at one-loop, only the terms with internal chirality change and complex g_L, g_R , or y_R, y_L , can give an imaginary part.

As seen in section 3.1, in 2HDMs, this is only possible at one-loop through a mixing scalar-pseudoscalar. At one loop, in the type X 2HDM, in the decoupling limit, $\cos(\beta - \alpha) \rightarrow 0$, where $M_{h_2} \simeq M_{h_3} \simeq M_A$ ¹⁷, using Eq. (13) and Eq. (48), we obtain,

$$\text{Im}\{C_{ii}^{2H}\} = \sum_a \frac{m_i Q_i \text{Im}\{(y_R^a)_{ii}(y_L^a)_{ii}^*\}}{M_{h_a}^2} I_2(x_{ia}) = \frac{g^2 m_i^3 Q_i}{2M_W^2} \epsilon \tan^2 \beta \left(\frac{I_2(x_{i2})}{M_{h_2}^2} + \frac{I_2(x_{i3})}{M_{h_3}^2} \right) \simeq -\frac{g^2 m_i^3}{4M_W^2} \frac{\epsilon \tan^2 \beta}{M_A^2} (3 + 2 \log(m_i^2/M_A^2)). \quad (94)$$

As expected, this contribution is suppressed by the lepton mass cube and this makes it too small. Numerically, for the electron, we have,

$$d_e = -\frac{e}{4\pi^2} \text{Im}\{C_{11}^{2H}\} \simeq -3 \times 10^{-21} \epsilon \frac{M_W^2 \tan^2 \beta}{M_A^2} \left(1 - \frac{\log(M_W^2/M_A^2)}{25} \right) \text{ e} \cdot \text{MeV}^{-1} \simeq -3 \times 10^{-31} \epsilon \frac{M_W^2 \tan^2 \beta}{M_A^2} \left(1 - \frac{\log(M_W^2/M_A^2)}{25} \right) \text{ e} \cdot \text{cm} \quad (95)$$

that, even if we assume $\epsilon \sim \mathcal{O}(1)$ is too small for the present experimental sensitivity. In type III 2HDM, using the Cheng-Sher ansatz, we would increase this contribution by a factor $m_\tau/m_e \simeq 3.5 \times 10^3$, assuming $\lambda_{ij} \sim \mathcal{O}(1)$. In these conditions, we would obtain a bound $\epsilon \lesssim 10^{-3}$ on the CP violating mixing.

¹⁶This is a rough estimate. The different numerical factor arises basically from the $g/2$ electroweak coupling and the signs in the different contributions [61].

¹⁷Here, M_A refers to the heavy masses in this limit, that would correspond to the pseudoscalar mass in the CP conserving limit

However, as for the anomalous magnetic moment, the main contribution in 2HDM comes from the Barr-Zee diagram. From Eq. (49), in the decoupling limit, we have,

$$d_e = -\frac{e}{4\pi^2} \text{Im} \{C_{11}^{\text{2HBZ}}\} \simeq -\frac{3e\alpha Q_u^2}{4\pi^2} \frac{g}{M_W} \epsilon \frac{\rho_{11}}{\sqrt{2}} \left(1 + \frac{m_t^2}{2M_{h_3}^2} \log^2 \frac{m_t^2}{M_{h_3}^2}\right) \simeq -3 \times 10^{-26} \epsilon \left(1 + \frac{m_t^2}{M_{h_3}^2} \log^2 \frac{m_t^2}{2M_{h_3}^2}\right) e \cdot \text{cm}, \quad (96)$$

where we assumed $\rho_{11}/\sqrt{2} \simeq m_e/v$, $\xi_i^u \simeq 1$ and used $\lim_{x_{i2} \rightarrow 0} f(x_{i2}) \simeq \lim_{x_{i3} \rightarrow 0} f(x_{i3}) \simeq \frac{1}{2} x_{i3} \log^2(x_{i3})$ and $f(x_{i1}) \simeq 1$ and slowly varying around $x_{i1} \simeq 1$. Therefore, the Barr-Zee diagram dominates the one-loop contribution to the electron EDM by approximately six orders of magnitude, giving a sizeable enhancement. As a result, this rough estimate suggests that scalar-pseudoscalar mixing, ϵ , would be constrained to be $\epsilon \lesssim 3 \times 10^{-4}$ by the present upper bound on $|d_e|$, considering only the top-quark loop. For a more detailed analysis within 2HDMs, see Ref. [40].

As we saw in the previous section, supersymmetric models can generate larger contribution, not suppressed by additional Yukawa couplings. Indeed, assuming an $O(1)$ phase in the μ parameter, appearing both in the chargino, Eq. (50) and the neutralino, Eq. (61), mass matrices, leads to the well-known Supersymmetric CP problem [71, 72].

If we consider the chargino contribution, from Eq. (59) we obtain,

$$d_e = -\frac{e}{4\pi^2} \text{Im} \{C_{11}^{\chi^\pm}\} \simeq \frac{e g^2 m_e}{4\pi^2 M_{\tilde{\nu}}^2} \text{Im} \{M_2 \mu\} \tan \beta \frac{I_2(\mu^2/M_{\tilde{\nu}}^2) - I_2(M_2^2/M_{\tilde{\nu}}^2)}{\mu^2 - M_2^2}, \quad (97)$$

which, in the limit $\mu \simeq M_2 \simeq M_{\tilde{\nu}}$ and using $I_2'(x) \xrightarrow{x \rightarrow 1} -1/4$, gives

$$d_e \simeq -\frac{e g^2 m_e}{16\pi^2 M_{\tilde{\nu}}^2} \frac{\text{Im} \{M_2 \mu\}}{M_{\tilde{\nu}}^2} \tan \beta \simeq 4 \times 10^{-24} \frac{M_W}{M_{\tilde{\nu}}^2} \sin \phi_\mu \tan \beta e \cdot \text{cm}. \quad (98)$$

where ϕ_μ is the relative phase between M_2 and μ in the basis off-diagonal and real charged-lepton masses. As a result, if we take $\sin \phi_\mu \sim O(1)$, the present electron EDM limit implies that the supersymmetric masses, $M_{\tilde{\nu}}$, must be larger than $\sim 80 \sqrt{\tan \beta}$ TeV, well above the electroweak scale. Alternatively, if we lower the sneutrino mass to $M_{\tilde{\nu}} \simeq 1$ TeV, we can an upper bound on the relative phase $\sin \phi_\mu \lesssim 1.4 \times 10^{-4} / \tan \beta$.

Clearly, these very strong constraints tell us that this μ parameter, must be (very approximately) real for masses near the electroweak scale. Indeed, this is a serious possibility, if we remember that the only observed phase in the Cabibbo-Kobayashi-Maskawa sector is associated to the flavor sector. Then, even assuming μ real, there are other phases in the MSSM that could contribute to EDMs [73–76].

Regarding contributions to EDM from extra $U(1)$ symmetries, given that flavor-diagonal gauge couplings are real, we must consider models with flavor off-diagonal couplings. The corresponding Wilson coefficient, given in Eq (72), is

$$d_e = -\frac{e}{4\pi^2} \text{Im} \{C_{11}^{Z'}\} \simeq \frac{e (g')^2}{4\pi^2} \sum_{k=2,3} \frac{2m_k}{M_{Z'}^2} \text{Im} \{(U^L)_{1k} (U^R)_{1k}^*\} \quad (99)$$

where we assumed $M_{Z'} \gg m_k$ and only the internal chirality changing contribution can be complex if right-handed and left-handed mixings are complex and different. In this expression there is an apparent enhancement, due the tau mass over the electron mass, but, as we saw explicitly in the supersymmetry case, in section 3.2, the smallness of the mixings can partially compensate this enhancement. Indeed, as shown in section 3.3, these off-diagonal couplings can come from the diagonalization of the Yukawa matrix in the presence extra scalars with non-vanishing $L_\mu - L_\tau$ charge. As a result, these couplings contribute to different flavor changing observables so that can be potentially strongly constrained. Therefore, they are expected to be small in full models. In addition to this presence of observable phases is also not trivial [77].

For the SMEFT analysis, the scenario is similar to the anomalous magnetic moment, with the difference that the NP scale that can be probed by the electron's EDM is much higher, due to the better sensitivity of the experiments. Indeed, with the same argument, we can estimate

$$\frac{\text{Im}[C_{eB}^{22}], \text{Im}[C_{eW}^{22}]}{\Lambda^2} \sim 10^{-12} \text{ TeV}^{-2}, \quad (100)$$

which is seven order of magnitude larger than Eq. (93). As a result, from Ref. [78], a larger class of operators is relevant, even if generated far above the TeV scale. In particular, beyond the tensor operators, sizable contributions may arise from Barr-Zee two-loop diagrams involving C_{eH} , as well as from NLO effects in the one-loop RGE of $C_{\text{lequ}(1)}$ with the top quark.

For a top-down analysis of potential NP contributions to EDMs in the context of scalar leptoquarks matched onto SMEFT operators, we refer the reader to [79].

For a review of EDMs contributions in these and other models, see Ref. [80].

4.3 Flavor-Changing Dipole Transitions

Flavor-changing dipole processes are among the most sensitive probes of physics beyond the SM. In the leptonic sector, the branching ratio $\text{BR}(\mu \rightarrow e\gamma)$ is among the most sensitive experimental observables for flavor-changing processes¹⁸. Indeed, after the discovery of neutrino

¹⁸ $\text{BR}(\mu \rightarrow eee)$ and μ - e conversion in nuclei are expected to reach comparable sensitivity in the near future [81–83]

oscillations, lepton flavor-violating transitions are expected in the SM with massive neutrinos. However, these contributions are extremely suppressed, well beyond the reach of current experiments, making any observed signal a clear indication of NP.

The analysis of different extensions of the SM that contribute to LFV follows the same strategy used in the previous sections. However, unlike the anomalous magnetic moments and EDMs, $\text{BR}(\mu \rightarrow e\gamma)$ is a directly measurable physical observable and, as such, is independent of the chosen basis. Nevertheless, it is often convenient to work in the basis where the charged lepton Yukawa matrix is diagonal and real, in which case, from Eq. (6), this observable is proportional to $|C_{21}|^2 + |C_{12}|^2$. Therefore, the main feature of extensions of the SM that contribute to $\text{BR}(\mu \rightarrow e\gamma)$ is the presence of additional flavor structures beyond the SM Yukawa matrices that are not simultaneously diagonalizable, giving rise to lepton flavor changing interactions.

Therefore, neglecting left-handed neutrino masses, in type I, II, X and Y 2HDM, all of which include a Z_2 symmetry that restricts each fermion species to couple to a single Higgs doublet, there are no contributions to $\mu \rightarrow e\gamma$. In type III 2HDM, and in the decoupling limit, from Eq. (43), we have,

$$\begin{aligned} C_{21} = C_{12}^* &= m_2 \rho_{k2}^* \rho_{k1} \left(\frac{I_1(m_k^2/M_H^2)}{2M_H^2} + \frac{I_1(m_k^2/M_A^2)}{2M_A^2} + \frac{J_1(m_k^2/M_{H^\pm}^2)}{M_{H^\pm}^2} \right) + m_k \rho_{2k} \rho_{k1} \left(\frac{I_2(m_k^2/M_H^2)}{2M_H^2} + \frac{I_2(m_k^2/M_A^2)}{2M_A^2} \right) \\ &\simeq m_2 (\rho_{12}^* \rho_{11} + \rho_{22}^* \rho_{21} + \rho_{32}^* \rho_{31}) \frac{1}{12M_A^2} - m_3 \rho_{23} \rho_{31} \frac{1}{M_A^2} \left(\frac{3}{2} + \log \frac{m_\tau^2}{M_A^2} \right). \end{aligned} \quad (101)$$

If we apply the Chang-Sher ansatz, this results in

$$C_{21} \simeq m_\mu \lambda_{32}^* \lambda_{31} \frac{m_\tau \sqrt{m_e m_\mu}}{24 M_W^2 M_A^2} - m_\tau \lambda_{23} \lambda_{31} \frac{m_\tau \sqrt{m_e m_\mu}}{2 M_W^2 M_A^2} \left(\frac{3}{2} + \log \frac{m_\tau^2}{M_A^2} \right), \quad (102)$$

and the branching ratio would be,

$$\text{BR}(\mu \rightarrow e\gamma) \simeq \frac{48}{\pi} \frac{m_e}{m_\mu} \frac{m_\tau^4}{M_A^4} \lambda_{23} \lambda_{31} \left(\frac{3}{2} + \log \frac{m_\tau^2}{M_A^2} \right)^2 \simeq 5.0 \times 10^{-9} \frac{M_W^4}{M_A^4} \lambda_{23}^2 \lambda_{31}^2 \left(1 - \frac{1}{6.15} \log \frac{M_W^2}{M_A^2} \right)^2 \quad (103)$$

From here, the present bound, $\text{BR}(\mu \rightarrow e\gamma) \leq 3.1 \times 10^{-13}$, would require $M_A \gtrsim 900$ GeV for $\lambda_{ij} \sim \mathcal{O}(1)$. Even in this case, the Barr-Zee diagram can provide an enhanced contribution. As the discussion is similar to that of the previous section, we refer to [35, 84] for further details on this contribution.

In supersymmetric models, slepton mass matrices provide additional flavor structures independent of the Yukawa matrices and we can expect contributions to the $\mu \rightarrow e\gamma$ process. If consider a general charged slepton mass matrix, the neutralino contribution to the C_{21} Wilson coefficient is,

$$C_{21}^{\chi^0} \simeq \frac{g^2}{2} \frac{m_\mu \mu \tan \beta}{M_{\tilde{l}_L}^2} \frac{(M_{\tilde{l}_L}^2)_{21}}{M_{\tilde{l}_L}^2} \left(M_1 t_W^2 \left(\frac{H(\mu^2/M_{\tilde{l}_L}^2) - H(M_1^2/M_{\tilde{l}_L}^2)}{\mu^2 - M_1^2} \right) - M_2 \left(\frac{H(\mu^2/M_{\tilde{l}_L}^2) - H(M_2^2/M_{\tilde{l}_L}^2)}{\mu^2 - M_2^2} \right) \right), \quad (104)$$

while,

$$C_{12}^{\chi^0} \simeq -g^2 \frac{m_\mu \mu \tan \beta}{M_{\tilde{l}_R}^2} \frac{(M_{\tilde{l}_R}^2)_{12}}{M_{\tilde{l}_R}^2} M_1 t_W^2 \left(\frac{H(\mu^2/M_{\tilde{l}_R}^2) - H(M_1^2/M_{\tilde{l}_R}^2)}{\mu^2 - M_1^2} \right), \quad (105)$$

We can make a simple estimate taking the limit of equal masses, $\mu \simeq M_1 \simeq M_2 \simeq M_{\tilde{l}_{L,R}}$, in the loop functions, $H'(1) = 1/15$. Then we get,

$$\begin{aligned} C_{21}^{\chi^0} &\simeq -\frac{g^2}{30} m_\mu \frac{M_2 \mu \tan \beta}{M_{\tilde{l}_L}^4} \frac{(M_{\tilde{l}_L}^2)_{21}}{M_{\tilde{l}_L}^2} \left(1 - \frac{M_1 t_W^2}{M_2^2} \right) \\ C_{12}^{\chi^0} &\simeq -\frac{g^2}{15} m_\mu \frac{M_1 t_W \mu \tan \beta}{M_{\tilde{l}_R}^4} \frac{(M_{\tilde{l}_R}^2)_{12}}{M_{\tilde{l}_R}^2}. \end{aligned} \quad (106)$$

The branching ratio is then [85],

$$\begin{aligned} \text{BR}(\mu \rightarrow e\gamma) &= \frac{3 \alpha_{\text{em}}}{\pi G_F^2 m_\mu^2} (|C_{22}|^2 + |C_{12}|^2) \simeq \frac{8 \alpha_{\text{em}}}{75 \pi} \frac{M_W^4 \mu^2 M_2^2 \tan^2 \beta}{M_{\tilde{l}}^8} \left(|(\delta_L^e)_{21}|^2 \left(1 - \frac{M_1 t_W^2}{M_2^2} \right)^2 + |(\delta_R^e)_{12}|^2 4 \frac{M_1^2 t_W^2}{M_2^2} \right) \\ &\simeq 4.5 \times 10^{-6} \left(\frac{500 \text{ GeV}}{M_{\tilde{l}}} \right)^4 \left(\frac{\tan \beta}{5} \right)^2 \left(|(\delta_L^e)_{21}|^2 (1 - t_W^2)^2 + |(\delta_R^e)_{12}|^2 4 t_W^2 \right), \end{aligned} \quad (107)$$

where we defined the MI as, $(\delta_{L,R}^e)_{ij} = (M_{\tilde{l}}^2)_{ij}/M_{\tilde{l}}^2$, and took all supersymmetric masses equal to $M_{\tilde{l}}$. The present bound on $\text{BR}(\mu \rightarrow e\gamma) < 3.1 \times 10^{-13}$, implies that for $M_{\tilde{l}} = 500$ GeV and $\tan \beta = 5$, we have $|(\delta_L^e)_{21}| \lesssim 3.4 \times 10^{-4}$ and $|(\delta_R^e)_{12}| \lesssim 2.7 \times 10^{-4}$. This means that the flavor structure in the slepton mass matrices can not be arbitrary and must be related with the flavor structure in the Yukawa matrices, perhaps by a flavor symmetry [73, 76].

Contributions to $\mu \rightarrow e\gamma$ from $U(1)'$ models are only possible in models with general flavor off-diagonal couplings. The Wilson coefficient is given in Eq (72). These contributions would be proportional to the off-diagonal Z' couplings, times a fermion mass. For instance,

taking the internal chirality changing contribution, that could be enhanced by the tau mass, we would have,

$$\begin{aligned} \text{BR}(\mu \rightarrow e\gamma) &= \frac{3\alpha_{\text{em}}}{\pi G_F^2 m_\mu^2} (g')^4 \frac{m_\tau^2}{M_{Z'}^4} 4 \left(|(U^L)_{23}(U^R)_{13}^*|^2 + |(U^R)_{23}(U^L)_{13}^*|^2 \right) \\ &\simeq 7.8 \times 10^4 \left(\frac{g'}{g} \right)^4 \left(\frac{M_W}{M_{Z'}} \right)^4 \left(|(U^L)_{23}(U^R)_{13}^*|^2 + |(U^R)_{23}(U^L)_{13}^*|^2 \right). \end{aligned} \quad (108)$$

Only from this process, assuming $g' \simeq g$, we would obtain, $|(U^L)_{23}(U^R)_{13}^*|, |(U^R)_{23}(U^L)_{13}^*| \leq 2 \times 10^{-9} (M_{Z'}/M_W)$.

Nevertheless, at this level, these off-diagonal are arbitrary and could only be defined in a complete model. In the example shown in section 3.3, these off-diagonal couplings are determined by the diagonalization of the Yukawa matrix in the presence extra scalars with non-vanishing $L_\mu - L_\tau$ charge and $(U^{L,R})_{23}$ or $(U^{L,R})_{13}^*$, are expected to be small.

Finally, the SMEFT approach allows us to estimate the sensitivity to the NP scale from the measurement of $\text{BR}(\mu \rightarrow e\gamma)$:

$$\frac{|C_{eB}^{21(12)}|, |C_{eW}^{21(12)}|}{\Lambda^2} \sim 10^{-10} \text{ TeV}^{-2}. \quad (109)$$

Therefore, when considering the first generations, the sensitivity to the off-diagonal dipole operators is nearly of the same order as to the imaginary part of the diagonal operator involving the first generation. Since the RGE is identical for all dipole operators, we will not discuss them further. It is, however, interesting to explore possible connections between the various observables, as they can be related by a flavor rotation. Indeed, if the NP allows for LFV, a misalignment between flavor and mass eigenstates can arise, leading to correlations among different observables. If we assume that the muon $g-2$ sensitivity is saturated by NP, or, seen in another way, that the discrepancy between the data-driven theoretical prediction and experiments is entirely due to NP, the present bound on $\text{BR}(\mu \rightarrow e\gamma)$ is such that [86]

$$|\epsilon_{12(21)}| \lesssim 10^{-5}; \quad \epsilon_{12(21)} = \frac{C_{eB}^{12(21)}}{\text{Re}[C_{eB}^{22}]}, \frac{C_{eW}^{12(21)}}{\text{Re}[C_{eW}^{22}]} \quad (110)$$

where ϵ_{ij} parametrize the flavor alignment.

5 Conclusions

The SM of particle physics has been tested with exceptional accuracy across a wide range of energy scales, becoming a well established theory for the description of fundamental interactions. However, it fails to explain several phenomena such as the nature of Dark Matter, the neutrino oscillations and the dominance of the matter of the antimatter. While the physics behind these processes may be at energy scale far beyond the reach of the present colliders, its effect could be indirectly detected in low energy experiments. Given the impressive sensitivity achieved in precision physics experiments, along with the expected improvements, it is worthwhile to explore how NP impacts one of the best tested observables: the dipole moments.

In this review, we presented a pedagogical analysis of the sensitivity of dipole transitions to NP beyond the SM, pointing out their intimate connection with the masses of SM fermions. We discussed why dipole-related observables are, and will likely remain in the foreseeable future, among the most sensitive probes of SM extensions.

As we have shown throughout this work, they offer insights into phenomena such as Lepton Flavor Violation, CP violation, and heavy particle dynamics, remaining at the forefront of efforts to uncover physics beyond the SM.

We provided general one-loop expressions for all dipole observables in terms of generic couplings, applicable to a wide range of models. Additionally, we examined the Barr-Zee two-loop contributions in the presence of new scalar interactions. These general results were then applied to a selected set of SM extensions, including two Higgs doublet models, supersymmetric frameworks, models with extra $U(1)$ symmetries, and SMEFT, to analyze the sensitivity of dipole observables to the masses and parameters of these theories.

In particular, for each of the three classes of observables studied, anomalous magnetic moments, electric dipole moments and Lepton Flavor Violation transitions, we focused on a particular generation, i.e. the one that we consider the most promising for the search of NP. Regarding the g -factor, we highlighted why the anomalous magnetic moment of the muon deserves special attention, since it is the most sensitive to NP and still presents some discrepancies between theory and experiments. For the EDMs, we focused on the electron one, whose upper bound is several orders of magnitude stronger than the other generations, and it is the most sensitive observable to NP. Finally, concerning Lepton Flavor Violation, we investigated the effects of beyond the SM physics on $\mu \rightarrow e\gamma$ transition, given its much stronger upper bounds than the other flavor transitions, and, in fact that is the only flavor violating observable currently searched for directly.

This work is only intended as an introductory review for readers arriving to the field for the first time, offering a selection of what we consider the most important concepts in the subject. It is meant to serve as a starting point, and we encourage interested readers to explore the extensive literature and existing reviews for a more in-depth understanding.

Acknowledgments

We would like to thank our collaborators on the topics discussed in this review, from whom we have learned much of what we present here, especially A. Masiero, L. Silvestrini, P. Paradisi, L. Calibbi, G.G. Ross, J. Jones-Pérez, M. Ardu, G. Barenboim, F.J. Botella, and many others. We acknowledge financial support from the Spanish Grant PID2023-151418NB-I00 funded by MCIU/AEI/10.13039/501100011033/ FEDER, UE and from Generalitat Valenciana projects CIPROM/2021/054 and CIPROM/2022/66.

References

- [1] B. Lee Roberts and William J. Marciano, editors. *Lepton dipole moments*, volume 20. 2009.
- [2] Friedrich Jegerlehner. *The Anomalous Magnetic Moment of the Muon*, volume 274. Springer, Cham, 2017.
- [3] Fred Jegerlehner and Andreas Nyffeler. The Muon $g-2$. *Phys. Rept.*, 477:1–110, 2009.
- [4] Peter Athron, Csaba Balázs, Douglas H. J. Jacob, Wojciech Kotlarski, Dominik Stöckinger, and Hyejung Stöckinger-Kim. New physics explanations of a_μ in light of the FNAL muon $g-2$ measurement. *JHEP*, 09:080, 2021.
- [5] E. D. Commins. Electric dipole moments of leptons. *Adv. At. Mol. Opt. Phys.*, 40:1–55, 1999.
- [6] Maxim Pospelov and Adam Ritz. Electric dipole moments as probes of new physics. *Annals Phys.*, 318:119–169, 2005.
- [7] Jonathan Engel, Michael J. Ramsey-Musolf, and U. van Kolck. Electric Dipole Moments of Nucleons, Nuclei, and Atoms: The Standard Model and Beyond. *Prog. Part. Nucl. Phys.*, 71:21–74, 2013.
- [8] Yoshitaka Kuno and Yasuhiro Okada. Muon decay and physics beyond the standard model. *Rev. Mod. Phys.*, 73:151–202, Jan 2001.
- [9] Lorenzo Calibbi and Giovanni Signorelli. Charged Lepton Flavour Violation: An Experimental and Theoretical Introduction. *Riv. Nuovo Cim.*, 41(2):71–174, 2018.
- [10] Marco Ardu and Gianantonio Pezzullo. Introduction to Charged Lepton Flavor Violation. *Universe*, 8(6):299, 2022.
- [11] Julian Schwinger. On quantum-electrodynamics and the magnetic moment of the electron. *Phys. Rev.*, 73:416–417, Feb 1948.
- [12] P. Kusch and H. M. Foley. The magnetic moment of the electron. *Phys. Rev.*, 74:250–263, Aug 1948.
- [13] X. Fan, T. G. Myers, B. A. D. Sukra, and G. Gabrielse. Measurement of the electron magnetic moment. *Phys. Rev. Lett.*, 130:071801, Feb 2023.
- [14] D. P. Aguillard et al. Measurement of the Positive Muon Anomalous Magnetic Moment to 0.20 ppm. *Phys. Rev. Lett.*, 131(16):161802, 2023.
- [15] T. Aoyama et al. The anomalous magnetic moment of the muon in the Standard Model. *Phys. Rept.*, 887:1–166, 2020.
- [16] A. Boccaletti et al. High precision calculation of the hadronic vacuum polarisation contribution to the muon anomaly. 7 2024.
- [17] Léo Morel, Zhibin Yao, Pierre Cladé, and Saïda Guellati-Khélifa. Determination of the fine-structure constant with an accuracy of 81 parts per trillion. *Nature*, 588(7836):61–65, 2020.
- [18] Richard H. Parker, Chenghui Yu, Weicheng Zhong, Brian Estey, and Holger Müller. Measurement of the fine-structure constant as a test of the standard model. *Science*, 360(6385):191–195, April 2018.
- [19] Maxim Pospelov and Adam Ritz. Ckm benchmarks for electron electric dipole moment experiments. *Phys. Rev. D*, 89:056006, Mar 2014.
- [20] Yasuhiro Yamaguchi and Nodoka Yamanaka. Large long-distance contributions to the electric dipole moments of charged leptons in the standard model. *Phys. Rev. Lett.*, 125:241802, Dec 2020.
- [21] Tanya S. Roussy, Luke Caldwell, Trevor Wright, William B. Cairncross, Yuval Shagam, Kia Boon Ng, Noah Schlossberger, Sun Yool Park, Anzhou Wang, Jun Ye, and Eric A. Cornell. An improved bound on the electron's electric dipole moment. *Science*, 381(6653):46–50, July 2023.
- [22] G. W. Bennett et al. An Improved Limit on the Muon Electric Dipole Moment. *Phys. Rev. D*, 80:052008, 2009.
- [23] K. Inami et al. An improved search for the electric dipole moment of the τ lepton. *JHEP*, 04:110, 2022.
- [24] K. Afanaciev et al. A search for $\mu^+ \rightarrow e^+ \gamma$ with the first dataset of the MEG II experiment. *Eur. Phys. J. C*, 84(3):216, 2024. [Erratum: *Eur. Phys. J. C* 84, 1042 (2024)].
- [25] Bernard Aubert et al. Searches for Lepton Flavor Violation in the Decays $\tau^+ \rightarrow e^+ \gamma$ and $\tau^+ \rightarrow \mu^+ \gamma$. *Phys. Rev. Lett.*, 104:021802, 2010.
- [26] M. J. Musolf and Barry R. Holstein. Observability of the anapole moment and neutrino charge radius. *Phys. Rev. D*, 43:2956–2970, May 1991.
- [27] F. J. Botella, M. Nebot, and O. Vives. Invariant approach to flavor-dependent CP-violating phases in the MSSM. *JHEP*, 01:106, 2006.
- [28] Lorenzo Calibbi, M. L. López-Ibáñez, Aurora Melis, and Oscar Vives. Muon and electron $g-2$ and lepton masses in flavor models. *JHEP*, 06:087, 2020.
- [29] Lorenzo Calibbi, M. L. López-Ibáñez, Aurora Melis, and Oscar Vives. Implications of the Muon $g-2$ result on the flavour structure of the lepton mass matrix. *Eur. Phys. J. C*, 81(10):929, 2021.
- [30] B. e. Lautrup, A. Peterman, and E. de Rafael. Recent developments in the comparison between theory and experiments in quantum electrodynamics. *Phys. Rept.*, 3:193–259, 1972.
- [31] Jacques P. Leveille. The Second Order Weak Correction to $(G-2)$ of the Muon in Arbitrary Gauge Models. *Nucl. Phys. B*, 137:63–76, 1978.
- [32] Kevin R. Lynch. General Prescriptions for One-loop Contributions to $a_{e,\mu}$. *Adv. Ser. Direct. High Energy Phys.*, 20:319–332, 2009.
- [33] Ta-Pei Cheng and Ling-Fong Li. *Gauge Theory of Elementary Particle Physics*. Oxford University Press, Oxford, UK, 1984.
- [34] Stephen M. Barr and A. Zee. Electric Dipole Moment of the Electron and of the Neutron. *Phys. Rev. Lett.*, 65:21–24, 1990. [Erratum: *Phys. Rev. Lett.* 65, 2920 (1990)].
- [35] D. Chang, W. S. Hou, and Wai-Yee Keung. Two loop contributions of flavor changing neutral Higgs bosons to $\mu \rightarrow e \gamma$. *Phys. Rev. D*, 48:217–224, 1993.
- [36] G.C. Branco, P.M. Ferreira, L. Lavoura, M.N. Rebelo, Marc Sher, and João P. Silva. Theory and phenomenology of two-Higgs-doublet models. *Physics Reports*, 516(1):1–102, 2012. Theory and phenomenology of two-Higgs-doublet models.
- [37] Alessandro Broggio, Eung Jin Chun, Massimo Passera, Ketan M. Patel, and Sudhir K. Vempati. Limiting two-Higgs-doublet models. *JHEP*, 11:058, 2014.
- [38] Johannes Haller, Andreas Hoecker, Roman Kogler, Klaus Mönig, Thomas Peiffer, and Jörg Stelzer. Update of the global electroweak fit and constraints on two-Higgs-doublet models. *Eur. Phys. J. C*, 78(8):675, 2018.
- [39] T. P. Cheng and Marc Sher. Mass Matrix Ansatz and Flavor Nonconservation in Models with Multiple Higgs Doublets. *Phys. Rev. D*, 35:3484, 1987.

- [40] Wolfgang Altmannshofer, Stefania Gori, Nick Hamer, and Hiren H. Patel. Electron edm in the complex two-higgs doublet model. *Physical Review D*, 102(11), December 2020.
- [41] Wolfgang Altmannshofer, Benoît Assi, Joachim Brod, Nick Hamer, J. Julio, Patipan Uttayarat, and Daniil Volkov. Electron EDM and $\Gamma(\mu \rightarrow e\gamma)$ in the 2HDM. 10 2024.
- [42] Stephen P. Martin. A Supersymmetry primer. *Adv. Ser. Direct. High Energy Phys.*, 18:1–98, 1998.
- [43] J. Hisano, T. Moroi, K. Tobe, and Masahiro Yamaguchi. Lepton flavor violation via right-handed neutrino Yukawa couplings in supersymmetric standard model. *Phys. Rev. D*, 53:2442–2459, 1996.
- [44] J. Hisano, T. Moroi, K. Tobe, Masahiro Yamaguchi, and T. Yanagida. Lepton flavor violation in the supersymmetric standard model with seesaw induced neutrino masses. *Phys. Lett. B*, 357:579–587, 1995.
- [45] Takeo Moroi. The Muon anomalous magnetic dipole moment in the minimal supersymmetric standard model. *Phys. Rev. D*, 53:6565–6575, 1996. [Erratum: *Phys.Rev.D* 56, 4424 (1997)].
- [46] Lawrence J. Hall, V. Alan Kostelecky, and S. Raby. New Flavor Violations in Supergravity Models. *Nucl. Phys. B*, 267:415–432, 1986.
- [47] F. Gabbiani, E. Gabrielli, A. Masiero, and L. Silvestrini. A Complete analysis of FCNC and CP constraints in general SUSY extensions of the standard model. *Nucl. Phys. B*, 477:321–352, 1996.
- [48] Andrzej J. Buras, Andrea Romanino, and Luca Silvestrini. $K \rightarrow \pi$ neutrino anti-neutrino: A Model independent analysis and supersymmetry. *Nucl. Phys. B*, 520:3–30, 1998.
- [49] G. Barenboim, C. Bosch, M. L. López-Ibañez, and O. Vives. Eviction of a 125 GeV "heavy"-Higgs from the MSSM. *JHEP*, 11:051, 2013.
- [50] Howard E. Haber and Gordon L. Kane. The Search for Supersymmetry: Probing Physics Beyond the Standard Model. *Phys. Rept.*, 117:75–263, 1985.
- [51] R. Foot, X.-G. He, H. Lew, and R. R. Volkas. Model for a lightz' boson. *Physical Review D*, 50(7):4571–4580, October 1994.
- [52] Wolfgang Altmannshofer, Chien-Yi Chen, P.S. Bhupal Dev, and Amarjit Soni. Lepton flavor violating z' explanation of the muon anomalous magnetic moment. *Physics Letters B*, 762:389–398, November 2016.
- [53] B. Grzadkowski, M. Iskrzynski, M. Misiak, and J. Rosiek. Dimension-Six Terms in the Standard Model Lagrangian. *JHEP*, 10:085, 2010.
- [54] Elizabeth E. Jenkins, Aneesh V. Manohar, and Michael Trott. Renormalization group evolution of the standard model dimension six operators ii: Yukawa dependence. *Journal of High Energy Physics*, 2014(1), January 2014.
- [55] Rodrigo Alonso, Elizabeth E. Jenkins, Aneesh V. Manohar, and Michael Trott. Renormalization group evolution of the standard model dimension six operators iii: gauge coupling dependence and phenomenology. *Journal of High Energy Physics*, 2014(4), April 2014.
- [56] Damir Bečirević, Ilja Doršner, Svjetlana Fajfer, Nejc Košnik, Darius A. Faroughy, and Olcyr Sumensari. Scalar leptoquarks from grand unified theories to accommodate the B -physics anomalies. *Phys. Rev. D*, 98(5):055003, 2018.
- [57] Bernat Capdevila, Andreas Crivellin, and Joaquim Matias. Review of semileptonic b anomalies. *The European Physical Journal Special Topics*, 233(2):409–428, December 2023.
- [58] Marco Ciuchini, E. Franco, G. Martinelli, L. Reina, and L. Silvestrini. Scheme independence of the effective Hamiltonian for $b \rightarrow s$ gamma and $b \rightarrow s$ g decays. *Phys. Lett. B*, 316:127–136, 1993.
- [59] Giuliano Panico, Alex Pomarol, and Marc Riembau. Eft approach to the electron electric dipole moment at the two-loop level. *Journal of High Energy Physics*, 2019(4), April 2019.
- [60] S. Navas et al. Review of particle physics. *Phys. Rev. D*, 110(3):030001, 2024.
- [61] K. Fujikawa, B. W. Lee, and A. I. Sanda. Generalized Renormalizable Gauge Formulation of Spontaneously Broken Gauge Theories. *Phys. Rev. D*, 6:2923–2943, 1972.
- [62] Jason Aebischer, Wouter Dekens, Elizabeth E. Jenkins, Aneesh V. Manohar, Dipan Sengupta, and Peter Stoffer. Effective field theory interpretation of lepton magnetic and electric dipole moments. *JHEP*, 07:107, 2021.
- [63] Athanasios Dedes and Howard E. Haber. Can the Higgs sector contribute significantly to the muon anomalous magnetic moment? *JHEP*, 05:006, 2001.
- [64] Martin Bauer and Matthias Neubert. Minimal Leptoquark Explanation for the $R_{D^{(*)}}$, R_K , and $(g-2)_\mu$ Anomalies. *Phys. Rev. Lett.*, 116(14):141802, 2016.
- [65] Oleg Popov and Graham A White. One Leptoquark to unify them? Neutrino masses and unification in the light of $(g-2)_\mu$, $R_{D^{(*)}}$ and R_K anomalies. *Nucl. Phys. B*, 923:324–338, 2017.
- [66] Andreas Crivellin, Dario Müller, and Toshihiko Ota. Simultaneous explanation of $R(D^{(*)})$ and $b \rightarrow \mu^+ \mu^-$: the last scalar leptoquarks standing. *JHEP*, 09:040, 2017.
- [67] Andrzej Czarnecki and William J. Marciano. The Muon anomalous magnetic moment: A Harbinger for 'new physics'. *Phys. Rev. D*, 64:013014, 2001.
- [68] A. D. Sakharov. Violation of CP Invariance, C asymmetry, and baryon asymmetry of the universe. *Pisma Zh. Eksp. Teor. Fiz.*, 5:32–35, 1967.
- [69] M. B. Gavela, P. Hernández, J. Orloff, and O. Pène. Standard model cp-violation and baryon asymmetry. *Modern Physics Letters A*, 09(09):795–809, 1994.
- [70] Patrick Huet and Eric Sather. Electroweak baryogenesis and standard model cp violation. *Phys. Rev. D*, 51:379–394, Jan 1995.
- [71] M. Dugan, Benjamin Grinstein, and Lawrence J. Hall. CP Violation in the Minimal N=1 Supergravity Theory. *Nucl. Phys. B*, 255:413–438, 1985.
- [72] Antonio Masiero and Oscar Vives. New physics in CP violation experiments. *Ann. Rev. Nucl. Part. Sci.*, 51:161–187, 2001.
- [73] Graham G. Ross, Liliana Velasco-Sevilla, and Oscar Vives. Spontaneous CP violation and nonAbelian family symmetry in SUSY. *Nucl. Phys. B*, 692:50–82, 2004.
- [74] L. Calibbi, J. Jones-Perez, and O. Vives. Electric dipole moments from flavoured CP violation in SUSY. *Phys. Rev. D*, 78:075007, 2008.
- [75] Junji Hisano, Minoru Nagai, and Paride Paradisi. Flavor effects on the electric dipole moments in supersymmetric theories: A beyond leading order analysis. *Phys. Rev. D*, 80:095014, 2009.
- [76] L. Calibbi, J. Jones-Perez, A. Masiero, Jae-hyeon Park, W. Porod, and O. Vives. FCNC and CP Violation Observables in a SU(3)-flavoured MSSM. *Nucl. Phys. B*, 831:26–71, 2010.
- [77] Andrzej J. Buras, Andreas Crivellin, Fiona Kirk, Claudio Andrea Manzari, and Marc Montull. Global analysis of leptophilic Z' bosons. *JHEP*, 06:068, 2021.
- [78] Marco Ardu and Nicola Valori. The equivalent Electric Dipole Moment in SMEFT. 3 2025.
- [79] W. Dekens, J. de Vries, M. Jung, and K. K. Vos. The phenomenology of electric dipole moments in models of scalar leptoquarks. *Journal of High Energy Physics*, 2019(1), January 2019.
- [80] Cari Cesarotti, Qianshu Lu, Yuichiro Nakai, Aditya Parikh, and Matthew Reece. Interpreting the Electron EDM Constraint. *JHEP*, 05:059, 2019.
- [81] K. Arndt et al. Technical design of the phase I Mu3e experiment. *Nucl. Instrum. Meth. A*, 1014:165679, 2021.

- [82] R. H. Bernstein. The Mu2e Experiment. *Front. in Phys.*, 7:1, 2019.
- [83] R. Abramishvili et al. COMET Phase-I Technical Design Report. *PTEP*, 2020(3):033C01, 2020.
- [84] Sacha Davidson. $\mu \rightarrow e\gamma$ in the 2HDM: an exercise in EFT. *Eur. Phys. J. C*, 76(5):258, 2016.
- [85] M. Ciuchini, A. Masiero, P. Paradisi, L. Silvestrini, S. K. Vempati, and O. Vives. Soft SUSY breaking grand unification: Leptons versus quarks on the flavor playground. *Nucl. Phys. B*, 783:112–142, 2007.
- [86] Gino Isidori, Julie Pagès, and Felix Wilsch. Flavour alignment of New Physics in light of the $(g - 2)_\mu$ anomaly. *JHEP*, 03:011, 2022.